Developmental Biology 329 (2009) 64–79

Contents lists available at ScienceDirect

Developmental Biology

journal homepage: www.elsevier.com/developmentalbiology

Functional redundancy of two *C. elegans* homologs of the histone chaperone Asf1 in germline DNA replication

Iwen F. Grigsby [1], Eric M. Rutledge, Christine A. Morton, Fern P. Finger *

Department of Biology and Center for Biotechnology and Interdisciplinary Studies, Rensselaer Polytechnic Institute, 110 8th St., Biotech-BCHM-2, Troy, NY 12180, USA

ARTICLE INFO

Article history:
Received for publication 19 September 2008
Revised 30 January 2009
Accepted 11 February 2009
Available online 20 February 2009

Keywords:
C. elegans
Asf1
unc-85
asfl-1
Sterility
Gametogenesis
Chromatin
Replication

ABSTRACT

Eukaryotic genomes contain either one or two genes encoding homologs of the highly conserved histone chaperone Asf1, however, little is known of their *in vivo* roles in animal development. UNC-85 is one of the two *Caenorhabditis elegans* Asf1 homologs and functions in post-embryonic replication in neuroblasts. Although UNC-85 is broadly expressed in replicating cells, the specificity of the mutant phenotype suggested possible redundancy with the second *C. elegans* Asf1 homolog, ASFL-1. The *asfl-1* mRNA is expressed in the meiotic region of the germline, and mutants in either Asf1 genes have reduced brood sizes and low penetrance defects in gametogenesis. The *asfl-1, unc-85* double mutants are sterile, displaying defects in oogenesis and spermatogenesis, and analysis of DNA synthesis revealed that DNA replication in the germline is blocked. Analysis of somatic phenotypes previously observed in *unc-85* mutants revealed that they are neither observed in *asfl-1* mutants, nor enhanced in the double mutants, with the exception of enhanced male tail abnormalities in the double mutants. These results suggest that the two Asf1 homologs have partially overlapping functions in the germline, while UNC-85 is primarily responsible for several Asf1 functions in somatic cells, and is more generally involved in replication throughout development.

Introduction

Histone chaperones are chromatin-associated proteins that assist in nucleosome formation and help mediate the post-translational modification of chromatin. These functions are important for replication, DNA repair and regulation of gene expression (Cheung et al., 2000). Among the most highly conserved histone chaperones are the Anti-silencing function 1 (Asf1) proteins. *ASF1* was originally isolated in budding yeast as a gene that derepresses the silent mating type locus when overexpressed (Le et al., 1997). Homologs from various organisms were subsequently demonstrated to function in critical cellular processes including chromatin assembly and disassembly (Adkins et al., 2004, 2007b; Galvani et al., 2008; Moshkin et al., 2002; Tyler et al., 1999), histone acetylation (Adkins et al., 2004, 2007a; Recht et al., 2006; Tsubota et al., 2007), DNA replication and repair (Chen et al., 2008; Franco et al., 2005; Grigsby and Finger, 2008; Groth et al., 2005, 2007; Le et al., 1997; Mello et al., 2002; Sanematsu et al., 2006; Schulz and Tyler, 2006; Sen and De Benedetti, 2006; Tyler et al., 1999), transcriptional regulation (; Adkins et al., 2004, 2007a; Sharp et al., 2001; Sutton et al., 2001; Zabaronick and Tyler, 2005), and cell cycle progression (Chen et al., 2008; Sanematsu et al., 2006; Tyler et al., 1999).

Although Asf1 is one of the most highly conserved histone chaperones, with either one or two isoforms found in eukaryotic genomes, little information is available as to their *in vivo* functions in animals, their expression patterns, and the roles of the different isoforms in those organisms with two Asf1 isoforms encoded in their genomes. The *Drosophila* genome contains a single *ASF1* gene, and the dASF1 protein localizes to replicating embryonic nuclei, indicative of its role in DNA replication (Bonnefoy et al., 2007; Moshkin et al., 2002). *Drosophila* ASF1 also participates in transcriptional regulation through interactions with the Brahma (SWI/SNF) chromatin-remodeling complex (Moshkin et al., 2002) and the Su(H)/H DNA binding protein complex (Goodfellow et al., 2007). There is evidence that the two human ASF1 isoforms have distinct, but overlapping roles *in vitro* and when expressed in yeast (Tamburini et al., 2005). Both human ASF1s are implicated in both DNA-dependent and DNA-independent histone H3 assembly pathways for DNA synthesis (Galvani et al., 2008; Tagami et al., 2004). However, only ASF1A is proposed to regulate the quiescence pathway in the presence of histone repression A factor (HIRA) (Zhang et al., 2005), while ASF1B is the sole Asf1 in the regulatory pathway directed by the transcription factor E2F during cell cycle progression (Hayashi et al., 2007).

The nematode *Caenorhabditis elegans* has two Asf1 homologs encoded in its genome (Grigsby and Finger, 2008). We previously found that *unc-85* encodes one of two worm Asf1 homologs (Grigsby and Finger, 2008). Mutations in *unc-85* cause variable post-embryonic cell division failures, primarily in terminal neuronal lineages, which result in defective locomotion and a reduced ability to mate and lay

* Corresponding author. Fax: +1 518 276 2851.
E-mail address: fingef@rpi.edu (F.P. Finger).
[1] Present address: Institute for Molecular Virology, 18-242 Moos Tower, 515 Delaware St. SE, Minneapolis, MN 55455, USA.

0012-1606/$ – see front matter © 2009 Elsevier Inc. All rights reserved.
doi:10.1016/j.ydbio.2009.02.015

embryos (Sulston and Horvitz, 1981). UNC-85 is widely expressed in replicating cells, where it localizes to nuclei, and in *unc-85* mutants, post-embryonic lineage failures in ventral cord neuroblasts arise during DNA replication (Grigsby and Finger, 2008). However, the contrast between the broad expression of *unc-85* in replicating cells and the specificity of the mutant phenotypes suggested that *unc-85* might be functionally redundant with the second *C. elegans* Asf1 homolog.

In the present study, we investigated the developmental functions of the second *C. elegans* Asf1 homolog, *asfl-1 (asf1-like)*, corresponding to sequence *C03D6.5*. The *asfl-1* gene is highly expressed in the meiotic region of the hermaphrodite germline. In contrast to *unc-85* mutants, no obvious phenotypes were observed in *asfl-1* mutants, except for a modest reduction in brood size. However, the *asfl-1; unc-85* double mutants were completely sterile, suggesting that UNC-85 and ASFL-1 have overlapping roles in the germline. Additionally, knockdown of *unc-85* in an *asfl-1* mutant background results in embryonic lethality. The sterility of the Asf1 double mutants results from germline replication failures, which result in abnormal chromatin and DNA damage, but not in apoptosis. Several somatic *unc-85* mutant phenotypes, including uncoordinated locomotion, are neither shared by nor modified in strains bearing mutations in *asfl-1*. The exception is the additional morphological defects of the male tail sensory rays observed in double mutants, but not in *unc-85* males. These results suggest that both of the *C. elegans* Asf1 homologs function to promote DNA replication in the germline, while UNC-85 is primarily responsible for several Asf1 functions in somatic cells, and is more generally involved in replication throughout development.

Materials and methods

Nematode strains and maintenance

All strains used in this study were derived from the Bristol strain N2 and were cultured using standard techniques on nematode growth medium (NGM) plates seeded with *E. coli* strain OP50 (Brenner, 1974). The following strains were used in this work: FX874 *asfl-1(tm874)* I; FX1625 *asfl-1(tm1625)* I; FX2812 *unc-85(tm2812)* II; MT319 *unc-85 (n319)* II; MT1065 *unc-85(n417)* II; CB1414 *unc-85(e1414)* II; NG3124 *dsh-2*(*or302*)/*mIn1*[*dpy-10*(*e128*) *mIs14*] II; FN57 [*asfl-1(tm874)I; unc-85(n319)*/*mIn1II*]. Strains FX874, FX1625 and FX2812 were kindly provided by S. Mitani and the National Bioresource Project, Tokyo Women's Medical University School of Medicine, Tokyo, Japan. Strains MT319 and MT1065 were kind gifts from H. R. Horvitz, Massachusetts Institute of Technology. Strain FN57 was created for this study (see below). All other strains were obtained from the *Caenorhabditis* Genetics Center. All mutant strains were backcrossed to N2 at least three times before use.

To obtain *unc-85(n319); asfl-1(tm874)* double mutants, strain FN57 [*asf-1(tm874); unc-85(n319)*/*mIn1*] was constructed as follows: FX874 males were crossed to NG3124 hermaphrodites, and their GFP-expressing male progeny were subsequently crossed with MT319 hermaphrodites. The F_1 hermaphrodite progeny from this second cross that expressed GFP, but appeared otherwise wild-type, were individually cultured. Their uncoordinated non-GFP-expressing progeny were scored and used as templates for single worm PCR assays (Fay, 2006) to confirm homozygosity of the *tm874* allele. FN57 hermaphrodites were heat shocked at 30 °C for 4 h, and the resulting male progeny were mated to FN57 hermaphrodites to obtain *unc-85 (n319); asfl-1(tm874)* males for use in analysis of male germlines and male tails.

Two alleles of *asfl-1* were used in this work: *tm874* deletes a 623 bp genomic region including the entire first exon and part of the second exon, and is predicted to be null; *tm1625* deletes 605 bp, including the entire first intron and the second exon (Fig. 1A), and is predicted to result in a frameshift resulting in a premature stop codon at residue 41. A third allele of *asfl-1, ok2060*, became available after we completed phenotypic characterization of the other two *asfl-1* alleles, and displayed very similar phenotypes (data not shown). Four alleles of *unc-85* were used in these studies. The *e1414* allele is a deletion of 142 nucleotides, resulting in a frameshift that produces a 132 residue truncated protein containing only the first 115 amino acids of the anti-silencing functional domain followed by 17 novel residues. The *n319* and *n471* alleles contain nonsense mutations at codons W41 and W154, respectively. The *e1414*, *n319* and *n471* alleles were previously characterized and shown to have significantly decreased *unc-85* mRNA expression (Grigsby and Finger, 2008). The *tm2812* allele deletes a genomic region spanning 206 bp in the second exon of *unc-85* and is predicted to be null. MT319 hermaphrodites were crossed to N2 males, and the heterozygous male progeny were mated to MT319 hermaphrodites to obtain *unc-85(n319)* males for analysis of the male germline and tail.

Confirmation of the exon–intron structure and 5′ UTR of asfl-1

Total RNAs from mixed developmental stages of N2s were prepared as previously described (Grigsby and Finger, 2008). SuperScript™ III Reverse Transcriptase (Invitrogen Corp., Carlsbad, CA) was used to generate first strand cDNAs using *asfl-1*-specific primers, according to the manufacturer's instructions. The first strand cDNAs were incubated with *E. coli* RNaseH (Invitrogen) at 37 °C for 20 min, then used as templates for PCR reactions with iProof high-fidelity DNA polymerase (Bio-Rad Laboratories, Hercules, CA). PCR products were purified using a PCR Cleanup Kit (Eppendorf AG, Hamburg, Germany), then sequenced (MacroGen, Rockville, MD). Sequences of primer sets are available upon request.

Brood size, egg-laying, and embryonic lethality assays

To determine brood sizes, ten worms from each strain analyzed (N2, MT319, FX2812, FX874, FX1625 and FN57) were individually plated, then transferred every 24 h to new plates. Each worm's progeny were counted daily until no further progeny were produced. We analyzed more *unc-85(tm2812)* worms ($n = 97$) than worms of the other strains because a small proportion (3%) die as later stage larvae, a phenotype not observed with the other three *unc-85* alleles. To determine whether animals lay embryos efficiently, ten L4 hermaphrodites of each strain (N2, FX2812, FX874, FX1625, MT319 and FN57) were individually plated, and the number of embryos laid was counted 24 h later.

Because *unc-85* mutants are defective in egg-laying (Sulston and Horvitz, 1981), the following method was used to analyze embryonic lethality: Gravid young adult hermaphrodites were placed in egg buffer (118 mM NaCl, 48 mM KCl, 2 mM $CaCl_2$, 2 mM $MgCl_2$, 25 mM Hepes, pH 7.3) and cut open at the vulva to release embryos, which were transferred onto NGM plates and counted. Embryo counting was repeated 24 h later to determine the number of unhatched embryos. At least 300 N2, MT319, FX874 and FX1625, and NG3124 embryos were analyzed. The progeny of *+/mIn1II* hermaphrodites, *asfl-1 (tm874)I; +/mIn1II* hermaphrodites, *unc-85(n319)/mIn1II* hermaphrodites, and *asfl-1(tm874)I; unc-85(n319)/mIn1II* hermaphrodites were similarly analyzed.

To assess whether the maternal Asf1 contribution was responsible for embryonic viability of the Asf1 mutants, RNAi of the Asf1 homologs was performed. Double stranded RNAs for *asfl-1* and *unc-85* were prepared as follows: A 345 bp SalI–HindIII restriction fragment of the *asfl-1* cDNA, and a 343 bp HincII–HindIII restriction fragment of the *unc-85* cDNA were each ligated into the dsRNA expression vector L4440 to create plasmids pCM75 and pCM90, respectively. These plasmids were then used as templates for *in vitro* production of dsRNAs using T7 RNA polymerase (New England Biolabs, Ipswich, MA) according to the supplier's recommendations.

The dsRNAs were purified by phenol–chloroform extraction and ethanol precipitation, then resuspended in TE. One gonad arm of N2, FX874, and MT319 young adult hermaphrodites were injected with 425 ng/μl *asfl-1* dsRNA and/or 612 ng/μl *unc-85* in DEPC-treated water (Invitrogen) water, or with DEPC-water alone (injection control). The numbers of worms injected for each experiment are: eight N2 injection control worms, nine N2s injected with *asfl-1* dsRNA, ten N2s injected with *unc-85* dsRNA, eight N2s injected with both *asfl-1* dsRNA and *unc-85* dsRNA, ten FX874 worms injected with *asfl-1* dsRNA, twelve FX874 worms injected with *unc-85* dsRNA, eleven MT319 worms injected with *asfl-1* dsRNA, and eight MT319 worms injected with *unc-85* dsRNA. Injected worms were moved to new plates every 24 h, and the number of dead embryos and viable worms was determined for each plate 24 h after the mother was shifted to a new plate.

Table 1
Asf1 mutant fertility phenotypes

Genotype	Brood size	Embryos laid 24 h post-L4
Wild-type	328 ± 5.1	46 ± 1.3
asfl-1(tm874)	273 ± 3.5[a,b,c]	35 ± 0.6[a,b,c]
asfl-1(tm1625)	264 ± 1.6[a,b,c]	38 ± 0.9[a,b,c]
unc-85(n319)	92 ± 6.3[a,c]	7 ± 1.6[a,c]
unc-85(tm2812)	61 ± 22.1[a,b]	22 ± 6.0[a,b]
asfl-1(tm874); unc-85(n319)	0	0

Data are averages ± SEM. For *unc-85(tm2812)*, $n = 97$. For all other strains, $n = 10$.
[a] Significantly different from wild-type, $P < 0.05$.
[b] Significantly different from *unc-85(n319)*, $P < 0.05$.
[c] Significantly different from *unc-85(tm2812)*, $P < 0.05$.

Quantitative RT-PCR

Embryos and staged worms (L1/L2, L3, L4, and young adults) were collected and total RNAs were extracted as described (Grigsby and Finger, 2008). For each sample, 100 ng of total RNA were used for reverse transcription and PCR using the SuperScript™ III Platinum® SYBR® Green One-Step qRT-PCR Kit (Invitrogen). *ama-1*, the gene encoding the largest subunit of *C. elegans* RNA polymerase II (Johnstone and Barry, 1996), was used as an endogenous standard. The *asfl-1* primers used in the real-time PCR reaction were 5′-ATGATGGGCAGGATGATGAC and 5′-TTCAGTATTGGGACCCGTCT; *ama-1* primers were 5′-ACGTCGCCTACCTACACTCCE and 5′-TACGTTGGC-GATGTTGGA. Experiments and data analysis were performed with a LightCycler® 480 Real-Time PCR Instrument and LightCycler® 480 Basic Software (Roche Applied Science, Indianapolis, IN).

RNA in situ hybridization

A reverse primer, 5′ TCATGTGCATTCGCCATTCGTTCGT, located in the fourth exon of *asfl-1* was used to synthesize the first strand cDNA with the SuperScript™ III Reverse Transcriptase (Invitrogen) as described above. The cDNA then served as a PCR template using *Taq* polymerase (Invitrogen) with a forward primer, 5′ TCTCGAATGG-GAATTGGTGTACG, located in the second exon and a reverse primer

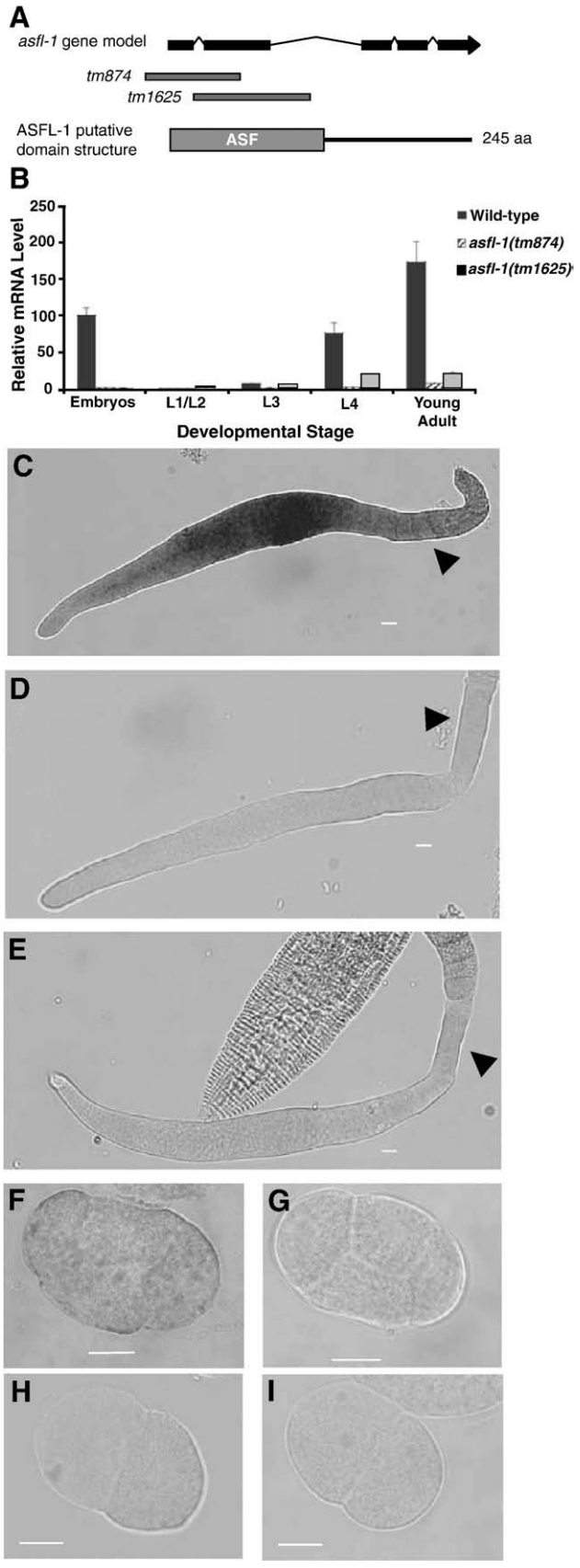

Fig. 1. (A) Gene structure of *asfl-1* and domain structure of ASFL-1. The intron–exon structure of *asfl-1* was confirmed by sequencing of the cDNA, and the corresponding domain architecture was predicted using NCBI's Conserved Domain Database. The anti-silencing functional domain is located in the N-terminus of ASFL-1 from M1 to P159 (Grigsby and Finger, 2008). Alleles *tm874* and *tm1625* bear genomic deletions (indicated by dashed bars) covering 623 bp and 605 bp, respectively. (B) Relative *asfl-1* mRNA expression levels during development measured by quantitative RT-PCR from wild-type, *asfl-1(tm874)*, and *asfl-1(tm1625)* worms. Results are normalized to expression levels in wild-type L1/2s ± standard deviation. RNA *in-situ* hybridization of dissected gonad arms (C–E) and embryos (F–I). In panels C–E, the distal end of the gonad is to the left, and in F–I, anterior is to the left. Panels C, E, F, and H, *asfl-1* antisense probe. Panels D, G, and I, *asfl-1* sense probe. (C, D) Wild-type dissected gonad arms. (E) A dissected *asfl-1(tm874)* gonad arm. Part of a worm carcass is seen above the dissected germline in panel E. (F, G) Wild-type four-cell embryos. (H, I) *asfl-1(tm874)* two-cell embryos. Scale bars are 10 μm.

located in the fourth exon of *asfl-1*. The PCR products were cloned into the PCR2.1 vector (Invitrogen) to create pFB67, and used as templates for preparation of digoxigenin (DIG) labeled anti-sense and sense DNA probes with DIG DNA Labeling Mix (Roche Applied Science, Indianapolis, IN). Probe synthesis and RNA *in situ* hybridization of dissected gonads and embryos were performed as described (Grigsby and Finger, 2008; Lee and Schedl).

Terminal deoxynucleotidyl transferase-mediated dNTP nick end-labeling (TUNEL) and SYTO-12 apoptosis assays

L4 worms were synchronized and cultured at 20 °C. Young adult worms were dissected 12 h later in PBS (200 mM sodium phosphate buffer, pH 7.2, 150 mM NaCl) containing 0.25 mM levamisole (Sigma-Aldrich Co., St. Louis, MO), and extruded gonads were fixed in PBS containing 4% paraformaldehyde for 20 min at room temperature. The TUNEL assay was performed as described (Parusel et al., 2006).

Apoptosis assays on 25 hermaphrodites of each genotype were performed using SYTO-12 (Invitrogen) as described (Gumienny et al., 1999) at 12 h and at 36 h post-L4.

Germ cells, sperm counts and fluorescence microscopy

To examine germ cell morphology, young adult hermaphrodites (12 h post-L4) were dissected and fixed as described above. For counting sperm, whole worms were fixed with Bouin's fixative as described (Nonet et al., 1997). After fixation, dissected gonads and whole animals were washed three times in PBSTx (PBS containing 0.5% Triton X-100) and stained with 1 μg/ml 4′-6-Diamidino-2-phenylindole (DAPI, Sigma-Aldrich Co.) for 10 min, washed twice in PBSTx, and mounted on slides (Duerr, 2006). A Zeiss LSM510 META confocal microscope equipped with C-Apochromat® 40×/1.2W Corr and plan-Apochromat® 63×/1.4 N.A. oil immersion objectives, and with a Zeiss AxioCam HRm digital CCD camera at 1× zoom, was used to collect 0.3 μm optical sections. The nuclear morphology of dissected germlines and the number of germ cells and sperm were determined from three-dimensional reconstructions created with the Zeiss LSM 510 software. Transmitted light differential interference contrast (DIC) images of dissected gonads or animals were obtained using a Zeiss Axiovert 200M inverted microscope equipped with plan-Apochromat® 40×/0.75 N.A., 63×/1.4 N.A. oil immersion objectives and a Zeiss AxioCam MRm digital CCD camera. At least 10 animals of each strain were analyzed.

In situ detection of germline DNA synthesis

Direct incorporation of Cy3-dUTP into germline nuclei was performed as described (Jaramillo-Lambert et al., 2007), except that the injection mix consisted of 50 μM Cy3-dUTP (Amersham Biosciences, Piscataway, NJ) in PBS, pH 7.2. After ~2.5 h of exposure to the Cy3-dUTP, gonads were dissected, fixed and DAPI stained as described (Jaramillo-Lambert et al., 2007). Optical sections of gonad arms were collected using a Zeiss LSM510 META confocal microscope equipped with a C-Apochromat® 40×/1.2W Corr objective. The total number of cells that incorporated Cy3-dUTP was determined for each dissected germline.

Analysis of male tail morphology, alae, and locomotory behavior

Ten young adult males of wild-type, *asfl-1(tm874)*, *unc-85(n319)* and *unc-85(n319); asfl-1(tm874)* genotypes were observed using the Zeiss Axiovert 200M microscope equipped with differential interference contrast optics and with a plan-Apochromat® 63×/1.4 N.A. oil immersion objective. Adult hermaphrodites of the same genotypes were observed in the same manner to determine the presence and appearance of the alae.

Thrashing assays (Miller et al., 1996) were performed as described on newly hatched larvae (Finger et al., 2003; Lickteig et al., 2001). At least ten worms of each strain (N2, FX2812, MT419, FN57) were examined.

Statistical analysis

All statistical tests were run using the InStat program (GraphPad Software Inc., LaJolla, CA). The Fisher's exact test with a two-sided *P* value was used to compare embryonic lethality data. One-way ANOVA with Newman–Keuls post hoc comparisons were performed on all other data. Significance was set at $P<0.05$.

Results

asfl-1 and unc-85 mutants have reduced brood sizes

The *C. elegans* genome contains two genes encoding homologs of the yeast histone chaperone Asf1 (Wormbase, 2005), *unc-85* (located on chromosome II) and *asfl-1* (located on chromosome I). The predicted Asf1 proteins encoded by these genes each contain a highly conserved amino-terminal anti-silencing domain (Conserved Domain Database, NCBI) and a more divergent carboxyl-terminal tail. We previously demonstrated that UNC-85 functions in post-embryonic neuroblast DNA replication (Grigsby and Finger, 2008). In order to learn more about the function of the second Asf1 homolog, ASFL-1, we first sequenced the *asfl-1* cDNA and confirmed the Wormbase predictions of the exon–intron structure and 5′ UTR (Wormbase, 2005) (Fig. 1A). The predicted ASFL-1 and UNC-85 proteins are highly similar (78% identical residues and 97% homologous residues), with most of the variation in the carboxyl-terminal tail domain (Grigsby and Finger, 2008).

To elucidate the developmental functions of *asfl-1*, strains bearing the *tm874* and *tm1625* alleles were characterized. The *tm874* allele deletes a 623 bp genomic region including the entire first exon and part of the second exon, and is predicted to be null, while *tm1625* deletes 605 bp, including the entire first intron and the second exon (Fig. 1A). No obvious morphological or behavioral defects were observed, however worms bearing either of these *asfl-1* mutations had slightly reduced brood sizes (~80% of wild-type; Table 1). We also determined that worms bearing either the *unc-85(n319)* or the *unc-85(tm2812)* mutations had brood sizes only 20–30% the size of wild-type broods (Table 1). These results suggested that both of the *C. elegans* Asf1 homologs might function in reproduction.

asfl-1 mRNA is expressed at relatively high levels in the germline and in early embryos

To determine the expression levels of *asfl-1*, quantitative RT-PCR (qRT-PCR) was performed on embryos and four different developmental stages of wild-type (N2) and *asfl-1* mutant worms. The qRT-PCR results were normalized to the expression level of wild-type L1/L2 larvae. In wild-type worms, relative *asfl-1* mRNA expression levels were high in embryos (16-fold, Fig. 1B), increased dramatically at the L4 (10-fold, Fig. 1B) and young adult stages (30-fold, Fig. 1B), indicating that *asfl-1* expression is developmentally regulated. In worms homozygous for either of the two *asfl-1* mutant alleles, overall expression remained low, reaching only 7–20% of the wild-type levels, and no relative increases in embryonic expression levels were observed (Fig. 1B). Because its mRNA expression level was the lower of the two *asfl-1* alleles tested (Fig. 1B), and the deletion eliminates the entire first exon including the start codon, the *tm874* allele was selected for more detailed analysis.

The slightly reduced brood size of the mutants and the *asfl-1* mRNA expression peak in young adults suggested that *asfl-1* might be expressed and function in the germline. The *C. elegans* gonad contains

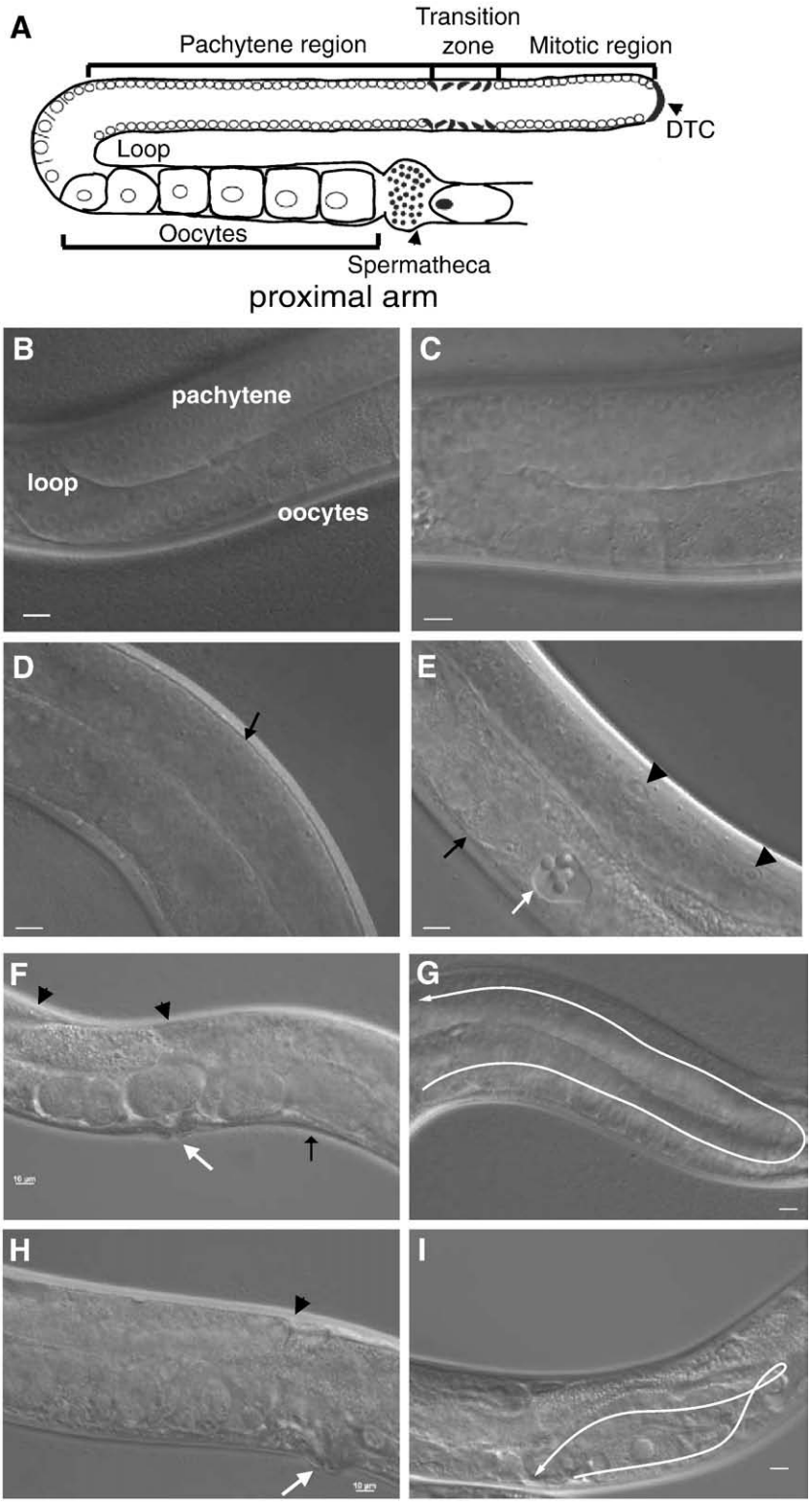

Fig. 2. Asf1 homologs are required in hermaphrodites for oocyte production and normal gonad morphology. (A) Schematic of an adult hermaphrodite gonad arm. (B–E) DIC images of gonad arms from young adult hermaphrodites. Panels B and C show focal planes at the surface of the germline in the pachytene region. (B) Wild-type. Nuclei in the pachytene region are uniformly sized. After passing through loop area, developing oocytes gradually enlarge and are arranged as a single row of cuboidal cells. (C) *asfl-1(tm874)* has germline morphology similar to wild-type. (D) A focal plane through the middle of an *unc-85(n319)* gonad arm to visualize the rachis with two rows of nuclei aligned along the periphery of the gonad arm (arrow). No abnormalities are observed. (E) *asfl-1(tm874); unc-85(n319)*. Abnormally enlarged germ cell nuclei are often observed (arrowheads), and oocytes are rounded, rather than the normal cuboidal shape (arrow). A vacuole is indicated (white arrow). (F, G) Wild-type gonad arms. (F) The distal tip cells (DTCs, arrowheads) are indicated and embryos (black arrow) are located within the uterus, near the vulva (white arrow). (G) A wild-type, U-shaped gonad arm. The direction of distal tip cell migration, inferred from the shape of the gonad arm, is indicated. (H) A gonad arm of an *asfl-1(tm874); unc-85(n319)* double mutant (similar focal plane as in A, arrowhead indicates DTC, white arrow indicates the vulva). No embryos are present. (I) An abnormally shaped gonad arm of an *asfl-1(tm874); unc-85(n319)* double mutant, with inferred distal tip cell migration path indicated. Scale bars are 10 μm.

two (anterior and posterior) symmetrical U-shaped arms which share a common uterus, diverging at their spermathecae, where sperm are stored (Hirsh et al., 1976; McCarter et al., 1999). Extension of the gonad arms begins in the L2 stage, and is led by distal tip cells (DTCs; Hall et al., 1999; Hedgecock et al., 1987). Germline nuclei exhibiting mitotic features can often be found in approximately the first 20 rows from the distal end (Crittenden et al., 1994). Upon exiting this region, germ cells progress through a narrow transition zone, where nuclei take on a characteristic crescent-shape as their chromatin begins to condense and early prophase I of meiosis is completed (Crittenden et al., 1994). Germ cells are in the pachytene stage of meiotic prophase from when they exit the transition zone until the loop area of the gonad arm, where oogenesis begins (Hirsh et al., 1976). To address whether *asfl-1* is expressed in the germline, *in situ* hybridizations to sense and antisense DNA probes derived from the *asfl-1* cDNA were performed on dissected gonad arms (Figs. 1C–E). We found that the *asfl-1* mRNA expression level was relatively low in the distal end of the germline in wild-type worms, increased gradually through the transition zone, and peaked in the pachytene region (Fig. 1C). Oocytes at diakinesis were also observed to express the *asfl-1* mRNA (Fig. 1C arrowhead). Expression of the *asfl-1* mRNA in embryos was also examined (Figs. 1F–I). Weak signals were detected in early embryos (Fig. 1F), but no signals were detectable past the 1.5-fold stage (data not shown). No mRNA expression was detected in *asfl-1(tm874)* dissected gonad arms (Fig. 1E) and embryos (Fig. 1G), consistent with the findings from qRT-PCR experiments that *asfl-1* mRNA expression was dramatically decreased in the mutants compared to wild-type young adults and embryos.

The two Asf1 homologs are required for fertility and normal gonad morphology

Although Asf1 histone chaperones are very highly conserved and function in critical processes, including replication, DNA repair, and regulation of transcription, the phenotypes of *asfl-1* and *unc-85* mutants are relatively mild, which led us to suspect that they might be partially functionally redundant. Double mutants were therefore constructed with the *asfl-1(tm874)* and *unc-85(n319)* alleles, as these are putative null alleles. We first tried to construct the double mutant by directly crossing *unc-85(n319)* hermaphrodites with *asfl-1 (tm874)* males, but the resulting double mutants were completely sterile, as well as uncoordinated. We then balanced *unc-85(n319)* with *mIn1* (Edgley and Riddle, 2001), crossed in *asfl-1(tm874)*, and again found that the *asfl-1(tm874); unc-85(n319)* progeny were viable, but uncoordinated and sterile, phenotypes commonly observed in mutants that are defective in post-embryonic and germline cell divisions (Albertson et al., 1978; Horvitz and Sulston, 1980; O'Connell et al., 1998; Sulston and Horvitz, 1981).

The reproductive systems of the *asfl-1(tm874)* and *unc-85(n319)* single mutants and of the double mutant were analyzed to determine the cause of the sterility. Hermaphrodite gonads from each single mutant appeared normal in morphology (Figs. 2C, D). However, *asfl-1 (tm874); unc-85(n319)* hermaphrodite gonads were often observed to contain unequally sized germ cell nuclei (Fig. 2E, arrowheads), and abnormal oocytes (Fig. 2E, black arrow), and never contained embryos (Fig. 2H). Normal, U-shaped gonad arms were observed in wild-type (Figs. 2B, F, G), *asfl-1(tm874)* (Fig. 2C), and *unc-85(n319)* hermaphrodites (Fig. 2D). In contrast, *asfl-1(tm874); unc-85(n319)* hermaphrodite gonad arms were generally small and variably misshapen (Fig. 2I).

Both C. elegans Asf1 homologs are required for normal oogenesis

The small size of the hermaphrodite germlines from the *asfl-1 (tm874); unc-85(n319)* double mutants (Figs. 2I and 3D) suggested that germ cell proliferation might be defective. To determine if this were the case, gonad arms from wild-type, *asfl-1(tm874)*, *unc-85 (n319)* and *asfl-1(tm874); unc-85(n319)* young adult hermaphrodites were dissected, DAPI-stained, and the number of germ cells in individual gonad arms were counted (Fig. 3E). The *asfl-1(tm874)* germlines (Figs. 3B, E) contained 27% fewer germ cells than wild-type worms (Figs. 3A, E). Although there was considerable variability within this genotype, the *unc-85(n319)* mutant germlines (Figs. 3C, E) contained an average of 36% fewer germ cells than wild-type germlines. The reductions in germ cell number observed with the individual Asf1 mutants were enhanced in the *asfl-1(tm874); unc-85(n319)* germlines (Figs. 3D, E), which contained 63% fewer germ cells than wild-type germlines. These results suggest that the two *C. elegans* Asf1 homologs have partially overlapping functions in germ cell proliferation.

To further understand the cause of the germ cell proliferation defect in the Asf1 mutants, germline chromatin was analyzed in DAPI-stained germlines dissected from wild-type, both single mutants, and the double mutant worms. In the loop region of the *C. elegans* germline, sister chromosomes are condensed and arranged at the periphery of

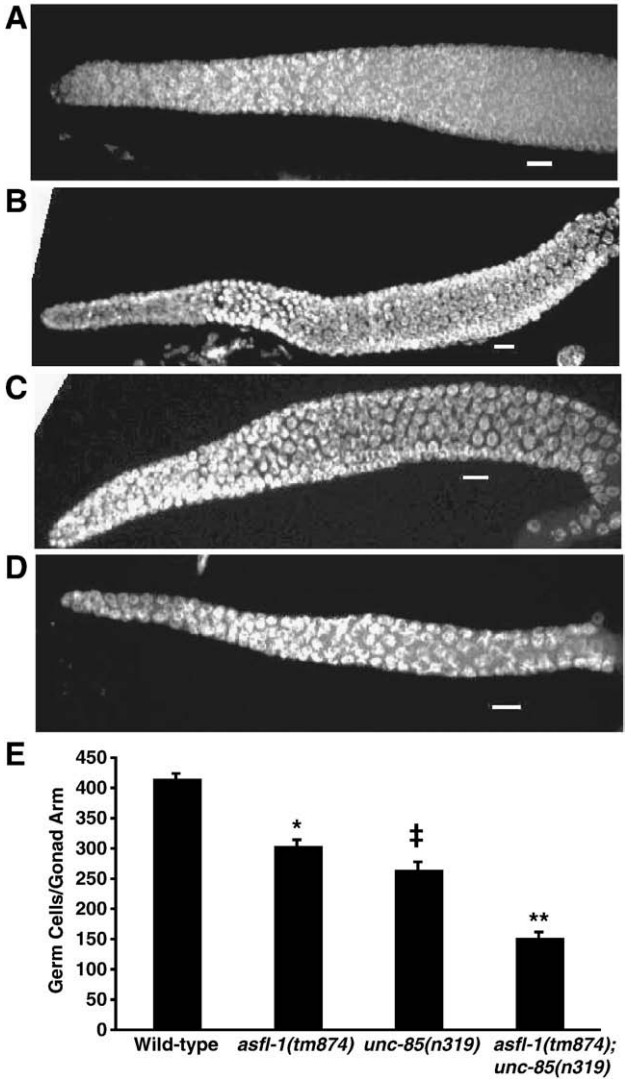

Fig. 3. Asf1 homologs are required for germ cell proliferation and hermaphrodite gametogenesis. (A–D) Dissected gonad arms stained with DAPI. Abundant nuclei can be observed in a wild-type gonad arm (A). Fewer germ cell nuclei are observed in gonad arms from *asfl-1(tm874)* (B) and *unc-85(n319)* (C). The germ cell population is greatly reduced in *asfl-1(tm874); unc-85(n319)* (D). (E) Mean number of germ cells per gonad arm ± standard errors of the mean (SEM) are shown for each strain examined, $n = 10$ for all strains except for *asfl-1(tm874); unc-85(n319)*, $n = 20$. *Significantly different from wild-type ($P < 0.001$), *unc-85(n319)* ($P < 0.01$) and *asfl-1(tm874); unc-85(n319)* ($P < 0.001$); ‡significantly different from wild-type ($P < 0.001$), *asfl-1(tm874)* ($P < 0.01$) and *asfl-1(tm874); unc-85(n319)* ($P < 0.001$); **significantly different from wild-type, *asfl-1(tm874* and *unc-85(n319)* (all P values < 0.001).

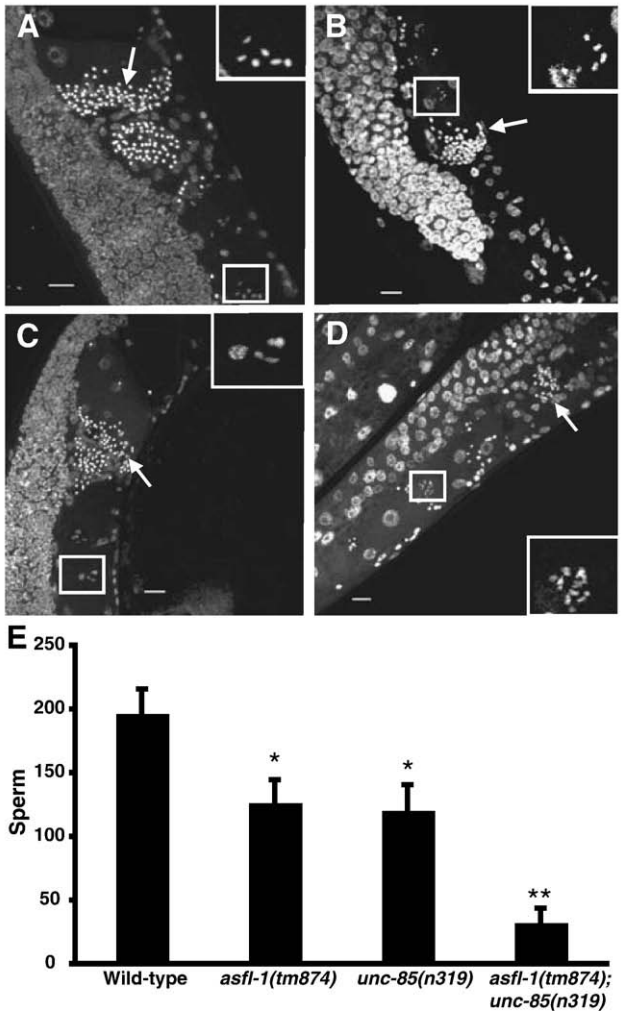

Fig. 4. Projections from confocal Z-series of DAPI-stained young adult hermaphrodite germlines from wild-type (A), *asfl-1(tm874)* (B), *unc-85(n319)* (C), and *asfl-1(tm874); unc-85(n319)* (D). The number of sperm (arrows) in the double mutants (D) is greatly reduced in comparison to the other strains. Boxes in panels A–D mark oocytes with bivalents arrested at diakinesis, with insets showing enlargements of the boxed areas. Fragmented chromosomes can be observed in *asfl-1(tm874)* (B) and in *asfl-1(tm874); unc-85(n319)* (D) oocytes. Additionally, the chromosomes in *unc-85(n319)* (C) are occasionally observed to not be fully condensed. Scale bars are 10 μm. (E) Reduced numbers of sperm are observed in the *asfl-1(tm874)*, *unc-85(n319)*, and *asfl-1(tm874); unc-85(n319)* hermaphrodites, compared to wild-type hermaphrodites. Means ± SEM are shown. *Significantly different from wild-type and *asfl-1(tm2812); unc-85(n319)*, $P<0.001$. **Significantly different from wild-type, *asfl-1(tm2812)*, and *unc-85(n319)*, $P<0.001$. Ten animals of each genotype were examined.

the nuclei as the germ cells progress from the late pachytene to the diplotene stages of meiosis I prophase (Hirsh et al., 1976). Between the loop region and the proximal region of the germline, germ cells proceed through the diplotene stage to diakinesis, with developing oocytes arranged in a single row and gradually enlarging as they move toward the proximal end of the germline (Fig. 2A) (Hirsh et al., 1976). Oocytes remain arrested in diakinesis of meiotic prophase I and do not complete meiosis until after fertilization (Hirsh et al., 1976). In wild-type worms (Figs. 4A and 5A, insets) and in *unc-85(n319)* mutants (Fig. 4C, inset), condensed chromosomes localized to the periphery of the germ cells, and six bivalents were present in oocytes, however the chromosomes in *unc-85(n319)* were not always fully condensed (Fig 4C, inset). In contrast, developing oocytes from *asfl-1(tm874)* mutants occasionally (13%, $n=15$) contained chromosomes with abnormal morphology (Fig. 4B, inset). Oocytes from *asfl-1(tm874); unc-85(n319)* double mutants rarely contained six bivalents, instead containing clumps of chromosomes, some of which appeared to be fragmented (Fig. 4D, inset). Germ cells containing disorganized chromosomes were almost always observed in the *asfl-1(tm874); unc-85(n319)* double mutants, particularly towards the proximal end of the pachytene region (Figs. 4D and 5J inset).

Because the germ cell chromatin often appeared abnormal in the double mutants, TUNEL assays were performed on dissected gonad arms to determine whether these abnormalities resulted in increased germ cell apoptosis. In contrast to wild-type (Fig. 5B) and to the single mutants (Figs. 5E, H), strong TUNEL signals were detected in the *asfl-1 (tm874); unc-85(n319)* double mutant germlines as the cells progressed from the pachytene to the diplotene stage of meiotic prophase (Fig. 5K). These results suggested that the absence of the *C. elegans* Asf1 homologs could result in germ cell apoptosis eliminating most potential oocytes, while the few remaining germ cells develop into oocytes with abnormal chromosome morphologies.

To test this hypothesis, we used SYTO-12 to stain apoptotic cells, and quantified the number of apoptotic germ cells in gonad arms from wild-type, *asfl-1(tm874)*, *unc-85(n319)* and *asfl-1(tm874); unc-85 (n319)* double mutant hermaphrodites. We found that at 12 h post-L4, the time at which we detected TUNEL staining of nuclei in the double-mutant germlines, there was essentially no SYTO-12 staining of the germlines of any of the strains tested. We repeated the SYTO-12 staining on worms at 36 h post-L4, the time at which this assay is generally performed, and found no significant differences between any of the tested strains. These results suggest that although the germ cell DNA of the double mutants contains numerous double-stranded breaks, the damage does not result in and is not caused by programmed cell death.

The C. elegans Asf1 homologs are required for spermatogenesis

After determining that oogenesis was defective in the *C. elegans* Asf1 double mutant hermaphrodites, we next investigated whether the Asf1 homologs also are required for spermatogenesis. To determine if there were defects in hermaphrodite spermatogenesis, the total number of spermatozoa within the spermathecae of wild-type, *unc-85(n319)*, *asfl-1(tm874)*, and *asfl-1(tm874); unc-85(n319)* young adult hermaphrodites were counted (Figs. 4A–D arrows and E). In each of the single mutants, the number of sperm was reduced by approximately 30–35% compared to wild-type. More severe effects were observed with *asfl-1(tm874); unc-85(n319)* hermaphrodites, which have only approximately 17% of the wild-type number of sperm, suggesting that the two Asf1 homologs function synergistically in hermaphrodite spermatogenesis.

While only approximately the first forty germ cells that enter meiosis in each gonad arm differentiate into hermaphrodite sperm, males generate sperm throughout their adult lives (L'Hernault, 1997). To determine if the *C. elegans* Asf1 homologs also function in male

Fig. 5. Loss of Asf1 homologs results in double-stranded breaks hermaphrodite germline DNA, but not in increased apoptosis. Panels A–L show projections of confocal Z-series of dissected gonad arms stained with DAPI, TUNEL, and merged images. The insets in A and J show enlargements of the boxed regions. (A–C) wild-type; (D–F) *asfl-1(tm874)*; (G–I) *unc-85(n319)*; (J–L) *asfl-1(tm874); unc-85(n319)*. No TUNEL signals are detected in the wild-type (B), *asfl-1(tm874)* (E), or *unc-85(n319)* (H) germlines. However, enhanced double-stranded DNA breaks, revealed by the TUNEL assays, are shown in the *asfl-1(tm874); unc-85(n319)* germlines (K), particularly at the proximal end of the pachytene region. While chromatin in wild-type pachytene germ cells is fairly uniform (inset A), germ cells with variably condensed chromatin (red arrows) are frequently observed in *asfl-1(tm874); unc-85 (n319)* double mutants (inset J). Scale bars are 10 μm. (M) Quantification of apoptotic cells in the germlines of adult hermaphrodites 12 h or 36 h post-L4 using SYTO-12 staining. Both gonad arms were examined for 25 animals of each genotype and condition. No increase in apoptosis is observed in any of the Asf1 mutant lines, suggesting that dsDNA breaks occur in the absence of programmed cell death.

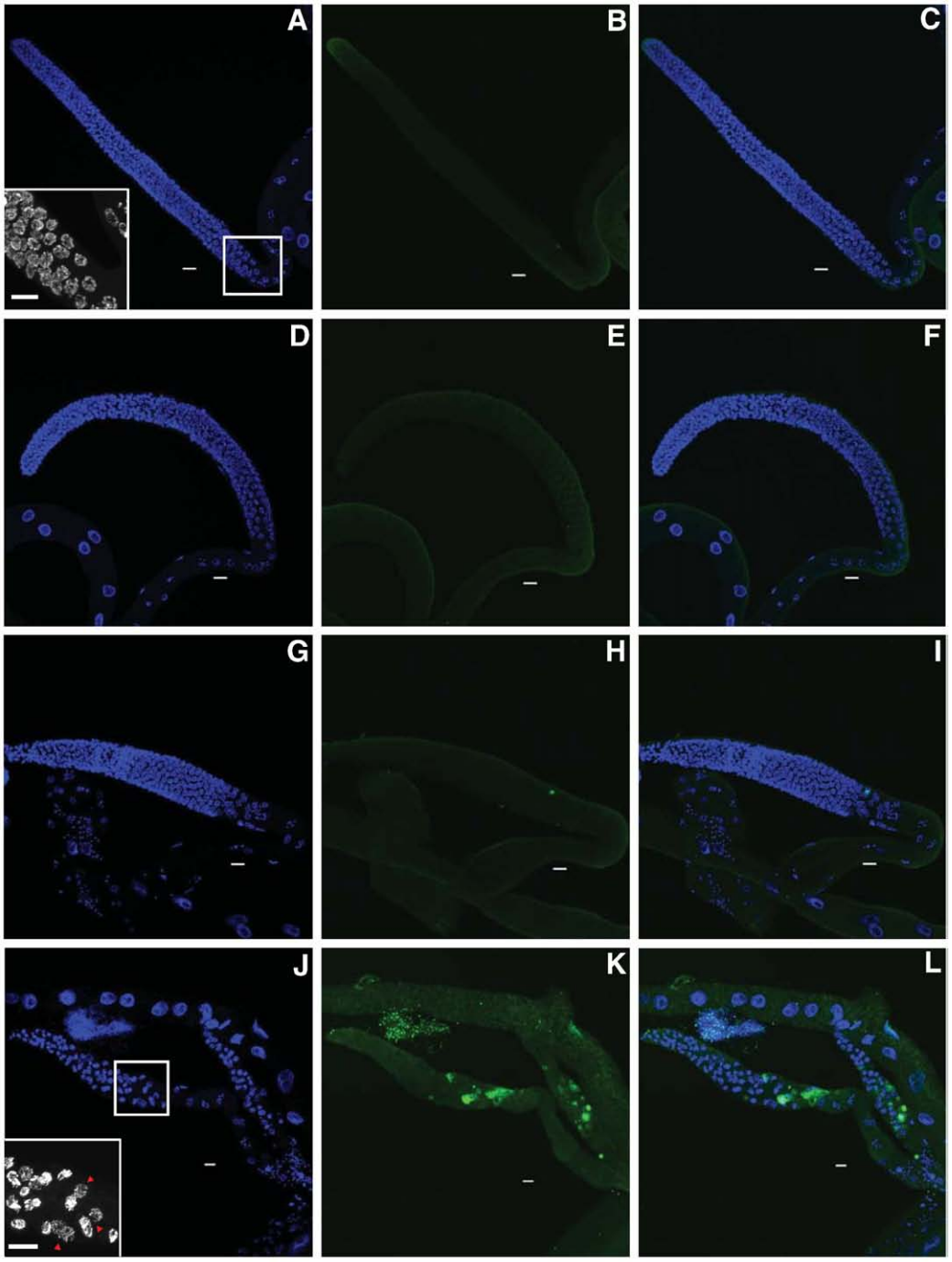
A
B
C
D
E
F
G
H
I
J
K
L
M
Apoptotic Cells
1
0.9
0.8
0.7
0.6
0.5
0.4
0.3
0.2
0.1
0
12 hours post L4
36 hours post L4
wild-type
asfl-1(tm874)
unc-85(n319)
asfl-1(tm874); unc-85(n319)

spermatogenesis, testes from wild-type, *unc-85(n319)*, *asfl-1(tm874)*, and double mutant males were examined. In wild type males, the proximal part of the germline contains pachytene nuclei, primary spermatocytes, secondary spermatocytes, and spermatids arrayed sequentially with each stage from pachytene to secondary spermatocytes progressively reduced in DNA content (Figs. 6A and B). Primary spermatocytes (4n) separate from the rachis, a central core of syncytial germline cytoplasm, prior to meiosis I and immediately undergo meiosis I, giving rise to secondary spermatocytes (2n), which then initiate meiosis II, producing spermatids (n) (Lints and Hall, 2005) (Fig. 6A). We used DAPI staining to distinguish between these stages and counted the primary spermatocytes and spermatids in

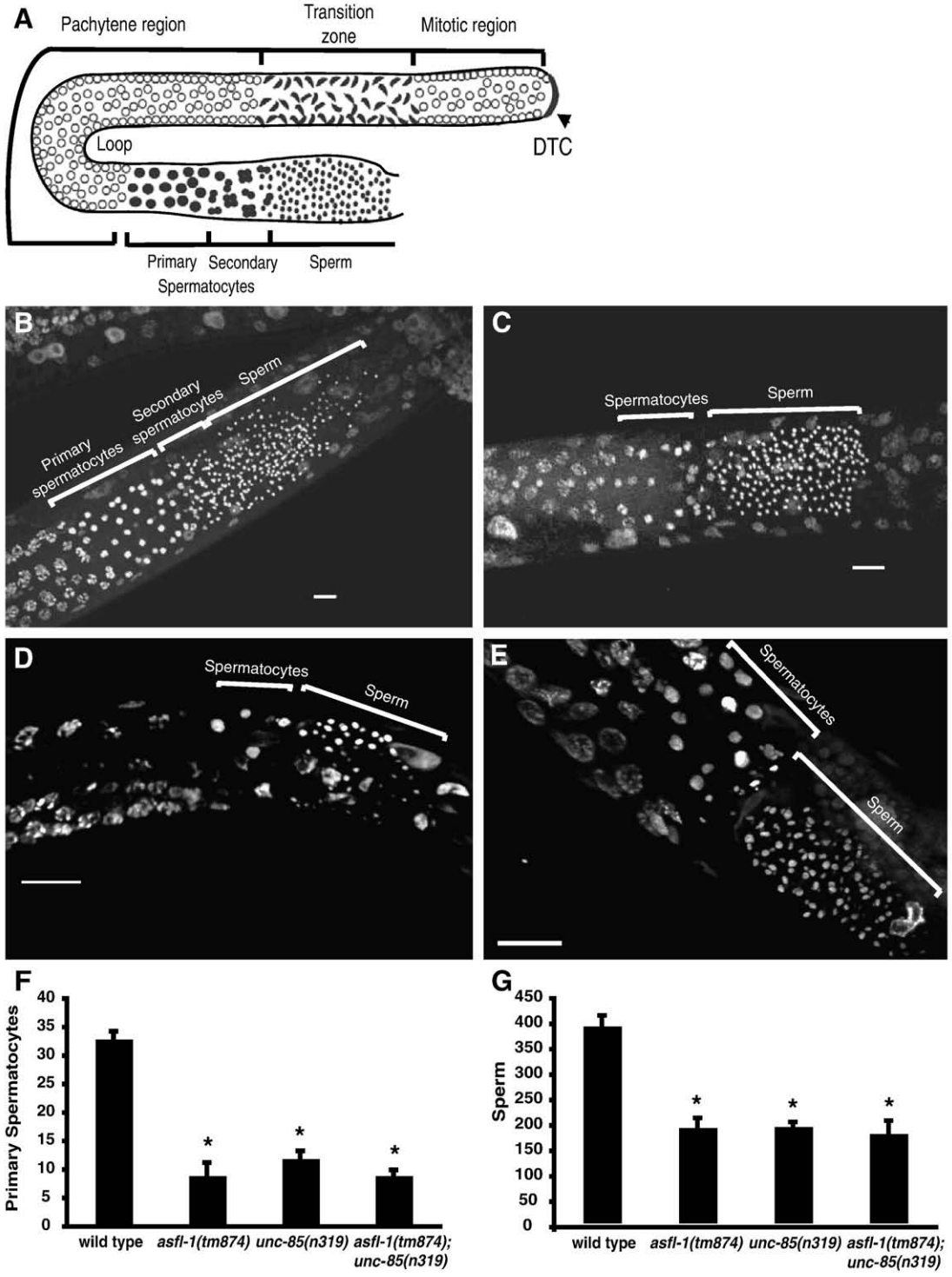

Fig. 6. Abnormal spermatogenesis in Asf1 mutant males. (A) Schematic of adult male germline. (B–E) Projections from confocal Z-series of DAPI-stained young adult male germlines. Scale bars are 10 μm. In the wild-type male germline, primary spermatocytes, secondary spermatocytes and sperm are sequentially arrayed, and can be distinguished by their relative DNA contents (B). Fewer spermatocytes and sperm are present in the germlines of *asfl-1(tm874)* (C), *unc-85(n319)* (D), and *asfl-1(tm874); unc-85(n319)* males (E). Reduced numbers of primary spermatocytes (F) and sperm (G) are observed in the *asfl-1(tm874)*, *unc-85(n319)*, and *asfl-1(tm874); unc-85(n319)* males, compared to wild-type males. Additionally, the sperm nuclei are irregular in morphology, suggesting a possible chromatin condensation defect. Means ± SEM are shown. *Significantly different from wild-type, $P<0.001$. Ten animals of each genotype were examined.

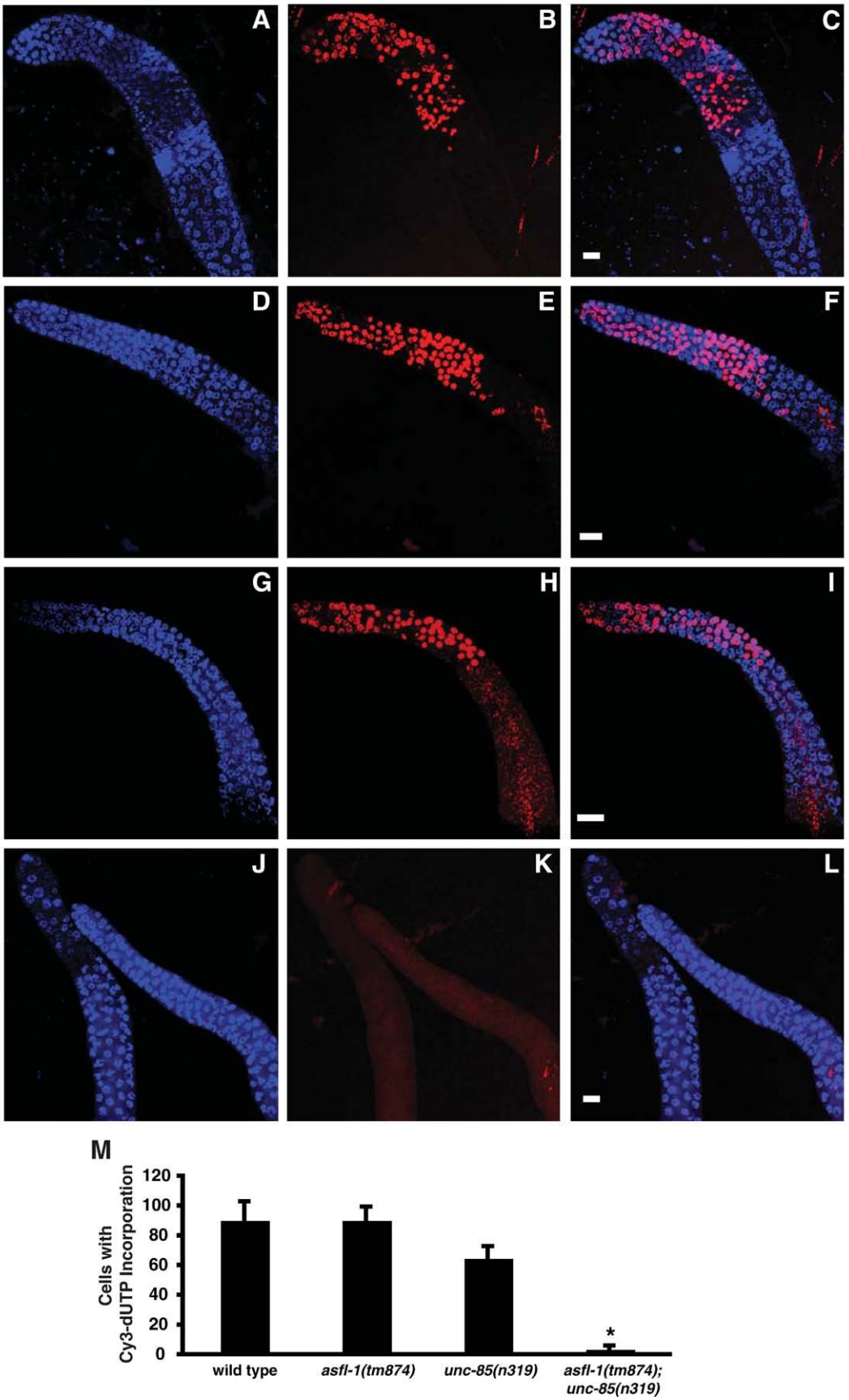

Fig. 7. Replication is blocked in *asfl-1(tm874); unc-85(n319)* germlines. Germlines from wild-type (A–C), *asfl-1(tm874)* (D–F), *unc-85(n319)* (G–I), and from *asfl-1(tm874); unc-85(n319)* (J–L) young adult hermaphrodites were directly injected with Cy3-dUTP, then allowed to recover for 2.5 h, before germlines were dissected, DAPI stained, and observed by confocal microscopy. (A, D, G, J) DAPI. (B, E, H, K) Cy3-dUTP incorporation. (C, F, I, L) Merge. Scale bars are 10 μm. (M) Quantification of Cy3-dUTP incorporation. The means of labeled nuclei per germline ± SEM are shown. *Significantly different from wild-type, $P<0.001$. $N=7$ for *asfl1(tm874)* and *asfl-1(tm874); unc-85(n319)*, and $N=8$ for wild-type and *unc-85(n319)*.

testes from wild-type, *asfl-1(tm874)*, *unc-85(n319)*, and *asfl-1 (tm874); unc-85(n319)* double mutant young adult males. Although its organization appeared normal, only nine primary spermatocytes on average were present in *asfl-1(tm874)* testes (Figs. 6C, F), a 73% decrease from the average of 33 primary spermatocytes present in wild-type testes (Figs. 6B, F). Only 12 primary spermatocytes on average were observed in the *unc-85(n319)* mutant testes, (Figs. 6D, F), 64% fewer than in wild-type testes. Testes from double mutant males resembled those from *asfl-1(tm874)* mutants, with an average of only nine primary spermatocytes (Figs. 6E, F). Furthermore, about 50% fewer spermatids were present in *asfl-1(tm874), unc-85(n319)* and *asfl-1(tm874); unc-85(n319)* testes than in wild-type testes (Fig. 6G), possibly because of the reduced number of primary spermatocytes. Germlines from *unc-85(n319)* males were occasionally disorganized, with sperm located in proximity to primary spermatocytes. A possible explanation for this phenotype is that copulatory apparatus defects of *unc-85* males (Sulston and Horvitz, 1981) (Fig. 8C) may result in sperm accumulation and germline disorganization. In addition to the decreased numbers of sperm in the double mutant, the few sperm have irregular nuclear morphology (Fig. 6E), suggesting that chromatin may not be properly condensed. Taken together, these results indicate that the Asf1 homologs participate in spermatogenesis in both sexes.

The Asf1 homologs function redundantly in germline DNA replication

Based on the known roles of Asf1s in other organisms (Franco et al., 2005; Groth et al., 2005; Kats et al., 2006; Le et al., 1997; Sanematsu et al., 2006; Schulz and Tyler, 2006; Tyler et al., 1999), and our previous finding that *unc-85* mutants are defective in post-embryonic replication (Grigsby and Finger, 2008), we hypothesized that the most critical function of the Asf1 homologs in the *C. elegans* germline might be in DNA replication. To test this hypothesis, we directly assessed incorporation of deoxyribonucleotides into germline DNA (Jaramillo-Lambert et al., 2007). Following direct injection of Cy3-dUTP into young adult hermaphrodite germlines, worms were allowed to recover for 2.5 h, and then their germlines were dissected, fixed, DAPI-stained, observed by confocal microscopy, and the number of nuclei that had incorporated Cy3-dUTP was quantified for each germline. There were no significant differences in the number of nuclei that incorporated Cy3-dUTP in germlines from wild-type (Figs. 7A–C, M), *asfl-1(tm874)* (Figs. 7D–F, M), and *unc-85(n319)* (Figs. 7G–I, M) hermaphrodites. In contrast, little to no incorporation of Cy3-dUTP (Figs. 7J–M) occurred in *asfl-1(tm874); unc-85 (n319)* hermaphrodite germlines. The double mutant germlines clearly contained Cy3-dUTP, and although it surrounded germ cell nuclei in the distal end of the germlines, confirming that the injections were successful, there was little colocalization with the DAPI staining. The DAPI-stained nuclei in the distal end of the *asfl-1 (tm874); unc-85(n319)* germlines sometimes appeared as enlarged, possibly interconnected masses of varying sizes, rather than the smaller, more uniformly-sized nuclei observed in the other strains analyzed, consistent with replication defects. These results demonstrate that germline DNA replication is blocked in the *asfl-1(tm874); unc-85(n319)* double mutants.

Table 2
Embryonic lethality of Asf1 homolog mutants

Genotype	Embryonic lethality (%)	*n*
Wild-type	0.4	711
asfl-1(tm874)I	5.6 [a]	304
asfl-1(tm1625)I	5.1 [a]	331
unc-85(e1414)II	3.9 [a]	356
unc-85(n319)II	4.6 [a]	325
unc-85(n471)II	4.7 [a]	384
unc-85(tm2812)II	2.9 [a]	315
+/mIn1II	2.9	302
asfl-1(tm874)I; +/mIn1II	11.0 [b]	309
unc-85(n319)/mIn1II	8.0 [b]	300
asfl-1(tm874)I; unc-85(n319)/mIn1II	14.7 [b]	347
Wild-type injection control	6.6±1.5	1322
asfl-1(RNAi)	7.9±2.3	1581
unc-85(RNAi)	11.2±2.8 [c]	859
asfl-1(RNAi); unc-85(RNAi)	8.3±1.7 [c]	1714
asfl-1(tm874)I; asfl-1(RNAi)	3.2±0.8	2140
asfl-1(tm874)I; unc-85(RNAi)	43.2±8.7 [d]	1234
asfl-1(RNAi); unc-85(n319)II	7.2±1.5 [c]	1394
unc-85(n319)II; unc-85(RNAi)	5.8±1.5	889

Strains above the double line were compared to wild-type and those below the double line were compared to *+/mIn1II*. Groups below the triple line were compared to the wild-type injection control.
[a]Significantly different from wild-type, $P \leq 0.002$.
[b]Significantly different from *+/mIn1II*, $P \leq 0.007$.
[c]Significantly different from *asfl-1(tm874)I; asfl-1(RNAi)*, $P \leq 0.05$.
[d]Significantly different from all other groups below triple line, $P \leq 0.002$.

Table 3
Locomotory behavior assays

Genotype	# of thrashes/2 min
Wild-type	152 ± 8.9
asfl-1(tm874)	152 ± 8.2
asfl-1(tm1625)	151 ± 7.0
unc-85(e1414)	102 ± 17.7[a]
unc-85(n319)	99 ± 9.2[a]
unc-85(n471)	101 ± 7.3[a]
asfl-1(tm874); unc-85 (n319)	116 ± 5.7[a]

Data are averages ± SEM. For all strains, $n = 10$.
[a] Significantly different from wild-type, *asfl-1(tm874)* and *asfl-1(tm1625)*, $P < 0.01$.

Asf1 function is required for embryo viability

Because the qRT-PCR results indicated that both genes are expressed at relatively high levels in embryos (Grigsby and Finger, 2008) (Fig. 1B), we examined whether mutations in either of the two Asf1 homologs affected embryonic viability (Table 2). Both of the *asfl-1* alleles and all four of the *unc-85* alleles tested conferred less than 6% embryonic lethality, indicating that the loss of each Asf1 homolog individually does not severely affect viability. Because the *asfl-1 (tm874); unc-85(n319)* double mutants are sterile, the viability of their progeny could not be assessed; however no synergistic effect on embryonic lethality was observed in the progeny of *asfl-1(tm874)I; unc-85(n319)II/mInI* hermaphrodites from the FN57 balanced strain compared to control *asfl-1(tm874)I; +/mInI* or *unc-85(n319)II/mInI* worms (Table 2). The viability of the *asfl-1(tm874); unc-85(n319)* double mutants may be due to maternal contributions from the balanced hermaphrodites, which is commonly observed in other *C. elegans* sterile uncoordinated mutants (O'Connell et al., 1998). Alternatively, the viability of the double mutants may be due to functional redundancy with other genes.

To determine if maternal Asf1 is necessary for embryo viability, dsRNA corresponding to *asfl-1* and/or to *unc-85* was injected into gonad arms of wild-type, *asfl-1(tm874), unc-85(n319)*, and the numbers of viable larvae and dead embryos from each injected mother were quantified (Table 2). Simultaneous RNAi of both Asf1s in a wild-type background did not reveal any increased embryonic lethality; however the efficiency of knockdown is known to be reduced when multiple genes are simultaneously targeted (Gonczy et al., 2000). Injection of *asfl-1* dsRNA into *unc-85* germlines also did not result in any increased embryonic lethality. The converse experiment, injection of *unc-85* dsRNA was injected into *asfl-1 (tm874)* germlines did result in a significant increase in embryonic lethality, consistent with the maternal contribution of Asf1 being necessary for embryonic development.

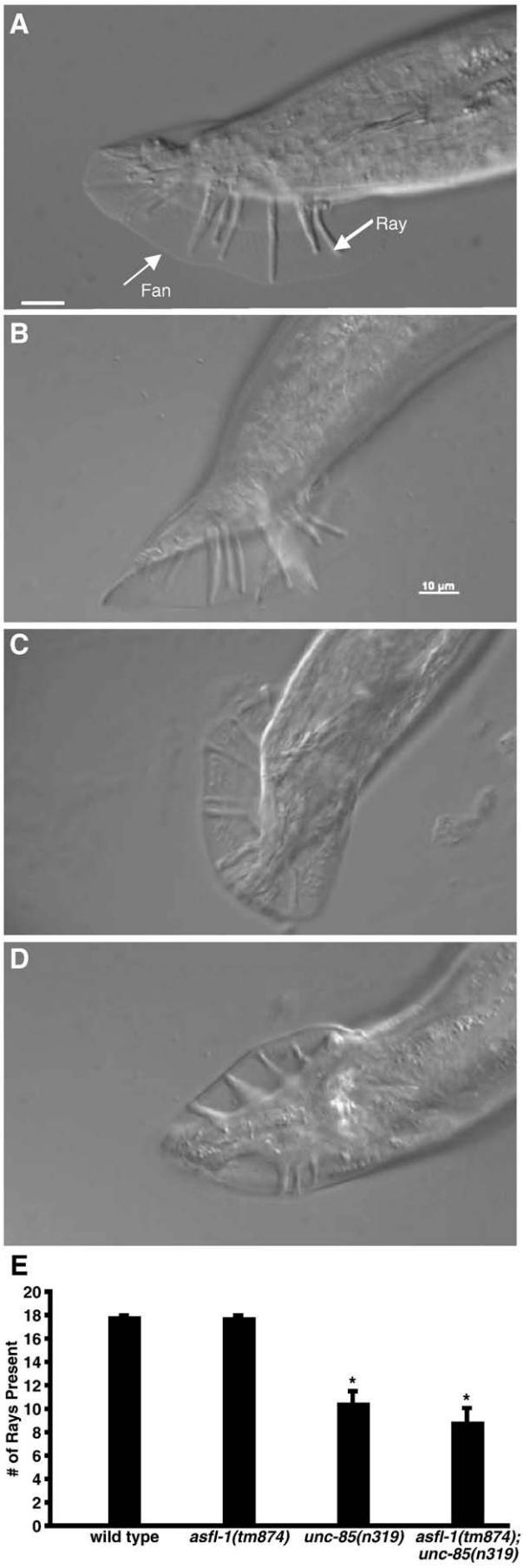

Requirements for Asf1 homologs in egg-laying, male tail development, and locomotion

All of the previously characterized *unc-85* mutant phenotypes arise from cell division failures during post-embryonic development and manifest during larval or adult life. These phenotypes include a reduced ability to lay embryos, morphological defects affecting the male copulatory apparatus, and uncoordinated locomotion (Sulston and Horvitz, 1981). We therefore examined these phenotypes in the Asf1 single and double mutant worms. Two *unc-85* mutants were found to retain embryos (Table 1), consistent with previous studies of *unc-85(e1414)* (Horvitz and Sulston, 1980; Sulston and Horvitz, 1981). Both of the *asfl-1* mutants tested also laid significantly fewer embryos than wild-type hermaphrodites, consistent with the reduced fertility of these worms (Table 1).

The *C. elegans* male tail contains a cuticular fan, in which nine pairs of sensory rays are embedded (Sulston et al., 1980). The ray neurons enable the male to respond to contact with the hermaphrodite and to turn when it encounters the end of the hermaphrodite prior to reaching the vulva (Liu and Sternberg, 1995). Examination of the tails of wild-type worms confirmed that all nine pairs of rays were present (Fig. 8A). The tails of *asfl-1(tm874)* males (Fig. 8B) resembled those of wild-type males, with all of the sensory rays generally present. Consistent with previous observations of missing rays in the tails of *unc-85(e1414)* males (Sulston and Horvitz, 1981), fewer rays were present in *unc-85(n319)* male tails (Fig. 8C). The *unc-85(n319); asfl-1(tm874)* male tails also had reduced numbers of sensory rays (Fig. 8D), resembling the tails of *unc-85* mutant males in ray number, however sensory rays often were observed to be wider than normal, suggesting that in addition to lineage defects, morphogenetic or cell identity defects resulting in ray fusions may have occurred. These results suggest that *unc-85* is the sole Asf1 homolog essential for normal egg-laying, and that both Asf1s may contribute to normal male tail morphology.

We previously determined that DNA replication failures are responsible for cell division failures in the post-embryonic ventral cord neuroblasts of *unc-85* mutants (Grigsby and Finger, 2008). To determine if UNC-85 and ASFL-1 function in other aspects of nervous system development or function, we assayed the locomotory behavior of newly hatched larvae (L1s). Post-embryonic neuroblast cell divisions do not begin until several hours post-hatching, allowing defects that occur as a result of post-embryonic cell division failures to be distinguished from those arising earlier in development. To assay locomotory behavior controlled by the ventral cord motor neurons, worms were placed in low-viscosity media, where they exhibit characteristic rapid, sequential thrashing (alternating body bends) (Chalfie and White, 1988). Determination of the number of times that a worm thrashes within a set time period allows quantification of locomotory defects (Miller et al., 1996). Thrashing assays of newly hatched L1s revealed that from 20–33% (depending on the allele) of *unc-85* mutant larvae are uncoordinated (Table 3). In contrast, *asfl-1* mutant larvae exhibited normal locomotion (Table 3). The *unc-85 (n319); asfl-1(tm874)* double mutant L1s were uncoordinated to a similar degree as *unc-85(n319)* mutants (Table 3), suggesting that only *unc-85* contributes to normal locomotion in newly hatched larvae.

Seam cells are lateral epidermal cells that produce the alae, longitudinal ridges of the lateral cuticle that are present in *C. elegans* in the L1, dauer, and adult stages. New seam cells are produced before each molt, and defects in seam cell division result in abnormalities, such as gaps in the alae (Sulston and Horvitz, 1981). Seam cell

Fig. 8. The copulatory apparatus is abnormal in *unc-85* mutant males. (A–D) DIC images of male tails. In both wild-type (A) and *asfl-1(tm874)* (B) males, nine pairs of rays are present in the fan. The *unc-85(n319)* male (C) is missing several rays (arrow), as is the *asfl-1(tm874); unc-85(n319)* double mutant male (D). In addition, some rays of the double mutant are wider than normal (D). Scale bar is 10 µm. (E) Quantification of number of rays per male tail. Ten animals of each genotype were examined and means ± SEM are shown. *Significantly different from wild-type, $P<0.001$.

divisions in *unc-85(e1414)* were previously reported to occur normally, and no alae defects were observed (Sulston and Horvitz, 1981). To determine if either or both of the *C. elegans* Asf1 homologs function in the seam cell divisions, the adult alae of wild-type, *asfl-1(tm874)*, *unc-85(n319)* and *unc-85(n319); asfl-1(tm874)* double mutant hermaphrodites were observed by DIC optics. The alae appeared to be normal in all of the strains (data not shown), suggesting that the Asf1 homologs may not be required for seam cell divisions.

Discussion

The genomes of many multicellular organisms, including *C. elegans*, *Homo sapiens*, *Mus musculus*, *Rattus norvegicus*, and *Arabidopsis thaliana* (Haas et al., 2002; Kawai et al., 2001; Munakata et al., 2000; The *C. elegans* Sequencing Consortium, 1998), contain two Asf1-encoding genes. All predicted Asf1 proteins are highly homologous, with most of the variation occurring in the carboxyl-terminal domain (Daganzo et al., 2003), and it is difficult to associate specific roles with primary amino acid sequence differences between Asf1 isoforms. Although much is known about the cellular functions of yeast Asf1, little is known about *in vivo* developmental functions for Asf1 homologs in more complex organisms, including whether (in those organisms with two Asf1s) each homolog has distinct and/or redundant roles. In this study, partially redundant functions in germline replication were elucidated for the two *C. elegans* Asf1 homologs, UNC-85 and ASFL-1, and several somatic functions were demonstrated to solely require UNC-85.

ASFL-1 and UNC-85 have partially redundant functions in germline DNA replication

The data presented here demonstrate that the two *C. elegans* Asf1 homologs have partially overlapping functions in germline replication. Mutations in either *asfl-1* or in *unc-85* result in reduced numbers of progeny compared to wild-type worms, the double mutants are completely sterile (Table 1), and injection of *asfl-1(tm874)* hermaphrodites with dsRNA for *unc-85* results in embryonic lethality in the progeny (Table 2). Germlines in each of the single mutants and in the double mutants contained fewer germ cells (Fig. 3E), and oogenesis, as well as both male and hermaphrodite spermatogenesis, was also defective in the mutants (Figs. 2–4 and 6). Moreover, abnormal gonad morphologies were observed only in the double mutants, and are likely to reflect defects in germ cell proliferation, although it is also possible that the two Asf1 homologs also function in cells of the somatic gonad, such as the distal tip cells (Hall et al., 1999; Hedgecock et al., 1987). Furthermore, TUNEL staining revealed extensive double-stranded breaks in DNA in the *asfl-1(tm874); unc-85(n319)* double mutants (Fig. 5K), although apoptosis assays were negative (Fig. 5M). A similar phenotype of extensive germline DNA breakage in the absence of apoptosis was previously reported for *C. elegans him-6 (e1104);top3α(RNAi)*, defective in a RecQ DNA helicase and in a topoisomerase III (Kim et al., 2002). The germ cells in *him-6(e1104); top3α(RNAi)* germlines were arrested in mitosis, and failed to enter into meiosis (Kim et al., 2002). Cognate pairs of RecQ DNA helicases and topoisomerase III are involved in a number of pathways important for genome stability, including in checkpoint signaling and as a checkpoint effector in response to DNA damage, and as a "dissolvasome", resolving structures created by homologous recombination (Mankouri and Hickson, 2007). This latter function is important for repair of ssDNA gaps, double-stranded DNA breaks, and stalled replication forks (Mankouri and Hickson, 2007). The similarity between the phenotypes of the Asf1 double mutant and loss-of-function in both *him-6* and *top-3α* may reflect their involvement in related functions in the germline.

The absence of apoptosis in the presence of extensive DNA damage in *C. elegans* Asf1 double mutants is somewhat surprising, as studies in other systems suggest a link between loss of Asf1 function and apoptosis. Cell death resembling apoptosis at G2/M was previously reported in a yeast *asf1* deletion mutant (Yamaki et al., 2001), and a recent study suggests that cells lacking *asf1* do not properly exit the DNA damage checkpoint after repair of damaged DNA is completed (Chen et al., 2008). Apoptosis also occurs in *Drosophila* loss-of-function mutants in the Tousled-like kinase, *tlk* (Carrera et al., 2003), and Asf1s from several organisms (Ehsan et al., 2004; Sillje and Nigg, 2001), including *Drosophila* (Carrera et al., 2003) and *C. elegans* (Han et al., 2005), are *in vitro* targets for TLK phosphorylation. However, our previous studies of replication failures in the post-embryonic ventral cord neuroblasts of *C. elegans* suggested that the replication failures do not always result in cell cycle arrest (Grigsby and Finger, 2008), which would be consistent with the failure to invoke a cell-cycle checkpoint leading to apoptosis.

Direct monitoring of germline DNA replication with microinjected Cy3-dUTP revealed little to no DNA synthesis in the *asfl-1(tm874); unc-85(n319)* double mutants (Fig. 7). Cy3 fluorescence was observed within the germlines of the double mutant, but only rarely coincided with the DAPI-stained germ cell DNA. These results indicate that replication in the germline is blocked, the most likely cause of the observed sterility of the *asfl-1(tm874); unc-85(n319)* double mutants (Table 1, Fig. 2H). DNA replication failures during the mitotic and/or meiotic cell cycles may result in daughter germ cells with unequal DNA content and chromosomes that would be unable to pair properly, leading to mitotic and/or meiotic cell division failures (Fig. 5K). These results are consistent with our previous findings that UNC-85 functions in DNA replication in post-embryonic neuroblast cell divisions (Grigsby and Finger, 2008). Furthermore, Asf1 proteins play critical roles during S phase in a variety of other organisms (Franco et al., 2005; Groth et al., 2005; Kats et al., 2006; Le et al., 1997; Sanematsu et al., 2006; Schulz and Tyler, 2006; Tyler et al., 1999). Additionally, RNA-mediated interference of the expression of both human Asf1 genes (hASF1B and hASF1B) in cultured human cells results in a much greater delay in S-phase than the knockdown of either single gene (Groth et al., 2005), suggesting that it may be a general phenomenon in organisms with two Asf1 homologs encoded in their genomes, that the two proteins have partially redundant functions in promoting DNA replication.

The precise roles for the worm Asf1 homologs in germline replication are not yet known, however there are clues from studies of Asf1 in other organisms. Yeast and *Drosophila* Asf1 homologs facilitate mitotic and meiotic S phase-associated acetylations of histone H3 (Adkins et al., 2007a; Driscoll et al., 2007; Fillingham et al., 2008; Han et al., 2007; Recht et al., 2006), and the *C. elegans* Asf1 homologs may similarly function to present histones to histone acetyltransferases. Yeast Asf1 also physically interacts *in vitro* with a replication fork component, replication factor C, and *ASF1* deletion mutants are unable to maintain several replication factors at stalled replication forks (Franco et al., 2005). *Drosophila* ASF1 is detected in replicating embryonic nuclei (Bonnefoy et al., 2007), and localizes to replication forks *in vivo* (Schulz and Tyler, 2006), while in cultured chicken cells, Asf1s are required for replication-coupled chromatin assembly and cell cycle progression (Sanematsu et al., 2006). Finally, RNAi depletion of human ASF1 blocks DNA unwinding at replication forks (Groth et al., 2007). These results suggest that Asf1 proteins play a direct role in replication, perhaps by helping to remove nucleosomes ahead of the replication fork, or by facilitating replication-coupled histone deposition.

Non-overlapping roles for the C. elegans Asf1 homologs in the germline

While our results demonstrate that Asf1 function is necessary for germline replication, the reduced brood sizes in each of the single mutants (Table 1) indicate that *unc-85* and *asfl-1* are not fully redundant in the germline. By qRT-PCR, *asfl-1* mRNA is primarily

expressed in adults and embryos (Fig. 1B), and results of *in situ* hybridization show that *asfl-1* mRNA is expressed at low levels in the distal end of the germline, where mitotic and meiotic DNA replication occurs, and is expressed more strongly in the pachytene region (Fig. 1C). In contrast, *unc-85* mRNA is highly expressed throughout the germline, and is expressed in many replicating cells throughout development (Grigsby and Finger, 2008). The expression patterns observed in *C. elegans* parallel observations of the mRNA expression patterns of the mouse Asf1 homologs, *CIA* and *CIA-II*. *CIA* is universally expressed in adult tissues, while *CIA-II* expression is largely restricted to testicular germ cells and the thymus, with lower expression levels in the small intestine and colon (Umehara and Horikoshi, 2003). These results suggest that the different expression patterns of the two *C. elegans* Asf1 homologs could underlie the phenotypic differences in their respective mutants. An alternative explanation is that their divergent C-terminal tails (Grigsby and Finger, 2008) provide functional specificity to UNC-85 and ASFL-1. There is also precedence for this in functional studies of the human Asf1s. Specialization of the two human Asf1s was observed when they each were expressed in a yeast Asf1 null mutant under the control of the yeast *ASF1* promoter to determine which yeast Asf1 functions could be complemented by each of the human genes (Tamburini et al., 2005). The hASF1A gene conferred resistance to DNA-damaging reagents, while hASF1B provided maintenance of genome stability during replication and transcriptional regulation (Tamburini et al., 2005). Other studies indicate that while hASF1A functions with HIRA in the quiescence pathway (Zhang et al., 2005), only hASF1B is regulated by the transcription factor E2F in human cell lines (Hayashi et al., 2007). However, these studies did not address developmental stage-specificity or tissue-specificity for the two human Asf1 homologs. Additionally, a functional proteomics study of substrates phosphorylated by the *C. elegans* mitogen activated protein kinase, *mpk-1*, identified ASFL-1, but not UNC-85, as a potential MPK-1 target (Lin and Reinke, 2008). MPK-1 functions in chromosome condensation and progression through the pachytene stage of meiosis I (Church et al., 1995), and ASFL-1 may function downstream of MPK-1 to regulate either or both of these functions.

In the *unc-85* mutants, somatic defects, rather than germline defects, may also contribute to the decreased brood size. The *unc-85* mutants are fertile, but display egg-laying defects (Sulston and Horvitz, 1981; Table 1) that result in the death of approximately 2/3 of hermaphrodites within 2–3 days post-L4, a time when wild-type hermaphrodites remain viable and continue reproduction. The high expression of *asfl-1* in the pachytene region (Fig. 1C) suggests that *asfl-1* may function to regulate gene expression necessary for progression through meiotic prophase. The absence of *asfl-1* would cause deregulated gene expression, resulting in delayed progression through meiosis, and in fewer germ cells.

Roles of the C. elegans Asf1 homologs during somatic development

In addition to the differences in germline expression patterns of the two Asf1 genes, and in the phenotypes of the mutants, our studies also suggest that the two *C. elegans* Asf1 homologs differ in their roles in somatic development. Previously identified somatic phenotypes of *unc-85* mutants (Grigsby and Finger, 2008; Sulston and Horvitz, 1981) including defective egg-laying, abnormal male tail morphology, and uncoordinated locomotion, are not observed in *asfl-1* mutants, and the double mutants resemble *unc-85* mutants (Tables 1 and 3, Fig. 8). We conclude that UNC-85 is the primary Asf1 involved in several somatic functions, including development and function of the ventral nerve cord and egg-laying. There are also missing sensory rays in *unc-85(n319)*, but not *asfl-1(tm874)* male tails. The defective egg-laying and male tail phenotypes are likely to result, at least in part, from cell division failures, as blocked ray and vulval lineages were previously observed in *unc-85(e1414)* mutants (Sulston and Horvitz, 1981). Although rays were also missing from the double mutant male tails, their abnormal morphologies suggest that ray fusions or other morphogenetic defects may have occurred in addition to lineage failures, and suggest the possibility of effects of Asf1 loss on gene expression. Some of the uncoordination observed in *unc-85* mutants is also likely to result from post-embryonic ventral nerve cord lineage failures (Grigsby and Finger, 2008; Sulston and Horvitz, 1981); however the impaired locomotory behavior observed in some newly hatched *unc-85* mutant larvae (Table 3) suggests that *unc-85* loss may also affect gene expression required for normal locomotion.

Observations of the alae in the *C. elegans* Asf1 single and double mutants suggest that some cell divisions may not require Asf1 function. The seam cells, specialized cells of the lateral epidermis, are born during embryonic development, and undergo post-embryonic cell divisions during each larval stage before fusing to form a syncytium in the mid-fourth larval stage. Alae are specializations of the lateral cuticle produced by the seam cells in the L1, dauer, and adult stages. Failed seam cell divisions result in defects in the alae, such as gaps (Sulston and Horvitz, 1981). No alae defects were observed in Asf1 single or double mutant adult hermaphrodites, suggesting that the seam cell divisions are not impaired. Since the double mutants are produced from a balanced line, maternally supplied Asf1 may be sufficient to support their seam cell divisions, although this would require the perdurance of maternally contributed Asf1 through four rounds of post-embryonic cell divisions occurring over 3.5 days. Alternatively, Asf1 function may not be required for successful replication in the seam cell lineages. Other classes of histone chaperones are encoded in the *C. elegans* genome, and may function in the seam cell lineages to load newly synthesized DNA with histones and regulate gene expression.

In conclusion, the expression pattern of *asfl-1* in the meiotic region of the germline, together with the phenotypic characterization of *asfl-1* single mutants and double mutants with *unc-85*, suggests that ASFL-1 may function primarily in the germline. In contrast, UNC-85 appears to be more ubiquitously involved in replication throughout development (Grigsby and Finger, 2008), although it is possible that some cell divisions may be Asf1-independent. The relatively weak germline phenotypes of the *asfl-1* and *unc-85* single mutants, in comparison to the strong germline replication defects and complete sterility of the double mutant, indicate that the two Asf1 homologs have partially overlapping functions in replication in the *C. elegans* germline. It will be interesting to learn if a similar division of roles between two Asf1 homologs is conserved in other organisms.

Acknowledgments

We thank Clayton Albracht for expert technical assistance, Bob Horvitz (Massachusetts Institute of Technology), Jonathan Hodgkin (Oxford University), Shohei Mitani (Tokyo Women's Medical College and the National Bioresource Project), and the *Caenorhabditis* Genetics Center (funded by the National Center for Research Resources) for providing some strains used in this work, and Yuji Kohara (National Institute of Genetics, Japan) for cDNAs. We are also grateful to Russ Ferland (Rensselaer Polytechnic Institute) for use of the AxioImager, Bob Palazzo (RPI) for use of MetaMorph, Chris Bjornsson (RPI) and Abby Dernburg (Lawrence Berkeley National Laboratory) for helpful discussions, the anonymous reviewers for helpful suggestions, and Russ Ferland and Andrea Page-McCaw (RPI) for critical reading of the manuscript. This research was funded by National Science Foundation Grant IOS-0745080 to F.P.F.

References

Adkins, M.W., Howar, S.R., Tyler, J.K., 2004. Chromatin disassembly mediated by the histone chaperone Asf1 is essential for transcriptional activation of the yeast PHO5 and PHO8 genes. Mol. Cell 14, 657–666.

Adkins, M.W., Carson, J.J., English, C.M., Ramey, C.J., Tyler, J.K., 2007a. The histone chaperone anti-silencing function 1 stimulates the acetylation of newly synthesized histone H3 in S-phase. J. Biol. Chem. 282, 1334–1340.
Adkins, M.W., Williams, S.K., Linger, J., Tyler, J.K., 2007b. Chromatin disassembly from the PHO5 promoter is essential for the recruitment of the general transcription machinery and coactivators. Mol. Cell. Biol. 27, 6372–6382.
Albertson, D.G., Sulston, J.E., White, J.G., 1978. Cell cycling and DNA replication in a mutant blocked in cell division in the nematode *Caenorhabditis elegans*. Dev. Biol. 63, 165–178.
Bonnefoy, E., Orsi, G.A., Couble, P., Loppin, B., 2007. The essential role of *Drosophila* HIRA for de novo assembly of paternal chromatin at fertilization. PLoS Genet. 3, 1991–2006.
Brenner, S., 1974. The genetics of *Caenorhabditis elegans*. Genetics 77, 71–94.
Carrera, P., Moshkin, Y.M., Gronke, S., Sillje, H.H., Nigg, E.A., Jackle, H., Karch, F., 2003. Tousled-like kinase functions with the chromatin assembly pathway regulating nuclear divisions. Genes Dev. 17, 2578–2590.
Chalfie, M., White, 1. G., 1988. The nervous system. In: Wood, W. (Ed.), The Nematode *Caenorhabditis elegans*. Cold Spring Harbor Laboratory, Cold Spring Harbor, New York, pp. 337–392.
Chen, C.C., Carson, J.J., Feser, J., Tamburini, B., Zabaronick, S., Linger, J., Tyler, J.K., 2008. Acetylated lysine 56 on histone H3 drives chromatin assembly after repair and signals for the completion of repair. Cell 134, 231–243.
Cheung, P., Allis, C.D., Sassone-Corsi, P., 2000. Signaling to chromatin through histone modifications. Cell 103, 263–271.
Church, D.L., Guan, K.L., Lambie, E.J., 1995. Three genes of the MAP kinase cascade, mek-2, mpk-1/sur-1 and let-60 ras, are required for meiotic cell cycle progression in *Caenorhabditis elegans*. Development 121, 2525–2535.
Crittenden, S.L., Troemel, E.R., Evans, T.C., Kimble, J., 1994. GLP-1 is localized to the mitotic region of the *C. elegans* germ line. Development 120, 2901–2911.
Daganzo, S.M., Erzberger, J.P., Lam, W.M., Skordalakes, E., Zhang, R., Franco, A.A., Brill, S.J., Adams, P.D., Berger, J.M., Kaufman, P.D., 2003. Structure and function of the conserved core of histone deposition protein Asf1. Curr. Biol. 13, 2148–2158.
Driscoll, R., Hudson, A., Jackson, S.P., 2007. Yeast Rtt109 promotes genome stability by acetylating histone H3 on lysine 56. Science 315, 649–652.
Duerr, J. S. (2006). Immunohistochemistry. In "WormBook" (The *C. elegans* Research Community, Ed.).
Edgley, M.L., Riddle, D.L., 2001. LG II balancer chromosomes in *Caenorhabditis elegans*: mT1(II;III) and the mIn1 set of dominantly and recessively marked inversions. Mol Genet Genomics 266, 385–395.
Ehsan, H., Reichheld, J. -P., Durfee, T., Roe, J.L., 2004. TOUSLED kinase activity oscillates during the cell cycle and interacts with chromatin regulators. Plant Physiol. 134, 1488–1499.
Fay, D. (2006). Genetic mapping and manipulation: Chapter 1—Introduction and basics. In "WormBook" (The *C. elegans* Research Community, Ed.).
Fillingham, J., Recht, J., Silva, A.C., Suter, B., Emili, A., Stagljar, I., Krogan, N.J., Allis, C.D., Keogh, M.C., Greenblatt, J.F., 2008. Chaperone control of the activity and specificity of the histone H3 acetyltransferase Rtt109. Mol. Cell. Biol. 28, 4342–4353.
Finger, F.P., Kopish, K.R., White, J.G., 2003. A role for septins in cellular and axonal migration in *C. elegans*. Dev. Biol. 261, 220–234.
Franco, A.A., Lam, W.M., Burgers, P.M., Kaufman, P.D., 2005. Histone deposition protein Asf1 maintains DNA replisome integrity and interacts with replication factor C. Genes Dev. 19, 1365–1375.
Galvani, A., Courbeyrette, R., Agez, M., Ochsenbein, F., Mann, C., Thuret, J.Y., 2008. In vivo study of the nucleosome assembly functions of ASF1 histone chaperones in human cells. Mol. Cell. Biol. 28, 3672–3685.
Gonczy, P., Echeverri, C., Oegema, K., Coulson, A., Jones, S.J., Copley, R.R., Duperon, J., Oegema, J., Brehm, M., Cassin, E., Hannak, E., Kirkham, M., Pichler, S., Flohrs, K., Goessen, A., Leidel, S., Alleaume, A.M., Martin, C., Ozlu, N., Bork, P., Hyman, A.A., 2000. Functional genomic analysis of cell division in *C. elegans* using RNAi of genes on chromosome III. Nature 408, 331–336.
Goodfellow, H., Krejci, A., Moshkin, Y., Verrijzer, C.P., Karch, F., Bray, S.J., 2007. Gene-specific targeting of the histone chaperone asf1 to mediate silencing. Dev. Cell 13, 593–600.
Grigsby, I.F., Finger, F.P., 2008. UNC-85, a *C. elegans* homolog of the histone chaperone Asf1, functions in post-embryonic neuroblast replication. Dev. Biol. 319, 100–109.
Groth, A., Ray-Gallet, D., Quivy, J.P., Lukas, J., Bartek, J., Almouzni, G., 2005. Human Asf1 regulates the flow of S phase histones during replicational stress. Mol. Cell 17, 301–311.
Groth, A., Corpet, A., Cook, A.J., Roche, D., Bartek, J., Lukas, J., Almouzni, G., 2007. Regulation of replication fork progression through histone supply and demand. Science 318, 1928–1931.
Gumienny, T., Lambie, E., Hartwieg, E., Horvitz, H., Hengartner, M., 1999. Genetic control of programmed cell death in the *Caenorhabditis elegans* hermaphrodite germline. Development 126, 1011–1022.
Haas, B.J., Volfovsky, N., Town, C.D., Troukhan, M., Alexandrov, N., Feldmann, K.A., Flavell, R.B., White, O., Salzberg, S.L., 2002. Full-length messenger RNA sequences greatly improve genome annotation. Genome Biol. 3 RESEARCH0029.
Hall, D.H., Winfrey, V.P., Blaeuer, G., Hoffman, L.H., Furuta, T., Rose, K.L., Hobert, O., Greenstein, D., 1999. Ultrastructural features of the adult hermaphrodite gonad of *Caenorhabditis elegans*: relations between the germ line and soma. Dev. Biol. 212, 101–123.
Han, Z., Riefler, G.M., Saam, J.R., Mango, S.E., Schumacher, J.M., 2005. The *C. elegans* Tousled-like kinase contributes to chromosome segregation as a substrate and regulator of the Aurora B kinase. Curr. Biol. 15, 894–904.
Han, J., Zhou, H., Li, Z., Xu, R.M., Zhang, Z., 2007. Acetylation of lysine 56 of histone H3 catalyzed by RTT109 and regulated by ASF1 is required for replisome integrity. J. Biol. Chem. 282, 28587–28596.
Hayashi, R., Goto, Y., Tanaka, R., Oonogi, K., Hisasue, M., Yoshida, K., 2007. Transcriptional regulation of human chromatin assembly factor ASF1. DNA Cell Biol. 26, 91–99.
Hedgecock, E.M., Culotti, J.G., Hall, D.H., Stern, B.D., 1987. Genetics of cell and axon migrations in *Caenorhabditis elegans*. Development 100, 365–382.
Hirsh, D., Oppenheim, D., Klass, M., 1976. Development of the reproductive system of *Caenorhabditis elegans*. Dev. Biol. 49, 200–219.
Horvitz, H.R., Sulston, J.E., 1980. Isolation and genetic characterization of cell-lineage mutants of the nematode *Caenorhabditis elegans*. Genetics 96, 435–454.
Jaramillo-Lambert, A., Ellefson, M., Villeneuve, A.M., Engebrecht, J., 2007. Differential timing of S phases, X chromosome replication, and meiotic prophase in the *C. elegans* germ line. Dev. Biol. 308, 206–221.
Johnstone, I.L., Barry, J.D., 1996. Temporal reiteration of a precise gene expression pattern during nematode development. EMBO J. 15, 3633–3639.
Kats, E.S., Albuquerque, C.P., Zhou, H., Kolodner, R.D., 2006. Checkpoint functions are required for normal S-phase progression in *Saccharomyces cerevisiae* RCAF- and CAF-I-defective mutants. Proc. Natl. Acad. Sci. U. S. A. 103, 3710–3715.
Kawai, J., Shinagawa, A., Shibata, K., Yoshino, M., Itoh, M., Ishii, Y., Arakawa, T., Hara, A., Fukunishi, Y., Konno, H., Adachi, J., Fukuda, S., Aizawa, K., Izawa, M., Nishi, K., Kiyosawa, H., Kondo, S., Yamanaka, I., Saito, T., Okazaki, Y., Gojobori, T., Bono, H., Kasukawa, T., Saito, R., Kadota, K., Matsuda, H., Ashburner, M., Batalov, S., Casavant, T., Fleischmann, W., Gaasterland, T., Gissi, C., King, B., Kochiwa, H., Kuehl, P., Lewis, S., Matsuo, Y., Nikaido, I., Pesole, G., Quackenbush, J., Schriml, L.M., Staubli, F., Suzuki, R., Tomita, M., Wagner, L., Washio, T., Sakai, K., Okido, T., Furuno, M., Aono, H., Baldarelli, R., Barsh, G., Blake, J., Boffelli, D., Bojunga, N., Carninci, P., de Bonaldo, M.F., Brownstein, M.J., Bult, C., Fletcher, C., Fujita, M., Gariboldi, M., Gustincich, S., Hill, D., Hofmann, M., Hume, D.A., Kamiya, M., Lee, N.H., Lyons, P., Marchionni, L., Mashima, J., Mazzarelli, J., Mombaerts, P., Nordone, P., Ring, B., Ringwald, M., Rodriguez, I., Sakamoto, N., Sasaki, H., Sato, K., Schonbach, C., Seya, T., Shibata, Y., Storch, K.F., Suzuki, H., Toyo-oka, K., Wang, K.H., Weitz, C., Whittaker, C., Wilming, L., Wynshaw-Boris, A., Yoshida, K., Hasegawa, Y., Kawaji, H., Kohtsuki, S., Hayashizaki, Y., 2001. Functional annotation of a full-length mouse cDNA collection. Nature 409, 685–690.
Kim, Y.C., Lee, M.H., Ryu, S.S., Kim, J.H., Koo, H.S., 2002. Coaction of DNA topoisomerase IIIalpha and a RecQ homologue during the germ-line mitosis in *Caenorhabditis elegans*. Genes Cells 7, 19–27.
L'Hernault, S.W., 1997. Spermatogenesis. In: Riddle, D.L., Blumenthal, T., Meyer, B.J., Priess, J.R. (Eds.), *C. elegans* II. Cold Spring Harbor Laboratory Press, Plainview, NY, pp. 271–294.
Le, S., Davis, C., Konopka, J.B., Sternglanz, R., 1997. Two new S-phase-specific genes from *Saccharomyces cerevisiae*. Yeast 13, 1029–1042.
Lee, M. -H., and Schedl, T. RNA in situ hybridization of dissected gonads. In "WormBook" (The *C. elegans* Research Community, Ed.), WormBook.
Lickteig, K.M., Duerr, J.S., Frisby, D.L., Hall, D.H., Rand, J.B., Miller 3rd, D.M., 2001. Regulation of neurotransmitter vesicles by the homeodomain protein UNC-4 and its transcriptional corepressor UNC-37/groucho in *Caenorhabditis elegans* cholinergic motor neurons. J. Neurosci. 21, 2001–2014.
Lin, B., Reinke, V., 2008. The candidate MAP kinase phosphorylation substrate DPL-1 (DP) promotes expression of the MAP kinase phosphatase LIP-1 in *C. elegans* germ cells. Dev. Biol. 316, 50–61.
Lints, R., and Hall, D. (2005). The Male Reproductive System Part III — The Germ line. In WormAtlas http://www.wormatlas.org/maleHandbook/ReprodMale_PartIII_Germ-Line.htm.
Liu, K.S., Sternberg, P.W., 1995. Sensory regulation of male mating behavior in *Caenorhabditis elegans*. Neuron 14, 79–89.
Mankouri, H.W., Hickson, I.D., 2007. The RecQ helicase-topoisomerase III-Rmi1 complex: a DNA structure-specific 'dissolvasome'? Trends Biochem. Sci. 32, 538–546.
McCarter, J., Bartlett, B., Dang, T., Schedl, T., 1999. On the control of oocyte meiotic maturation and ovulation in *Caenorhabditis elegans*. Dev. Biol. 205, 111–128.
Mello, J.A., Sillje, H.H., Roche, D.M., Kirschner, D.B., Nigg, E.A., Almouzni, G., 2002. Human Asf1 and CAF-1 interact and synergize in a repair-coupled nucleosome assembly pathway. EMBO Rep. 3, 329–334.
Miller, K.G., Alfonso, A., Nguyen, M., Crowell, J.A., Johnson, C.D., Rand, J.B., 1996. A genetic selection for *Caenorhabditis elegans* synaptic transmission mutants. Proc. Natl. Acad. Sci. U. S. A. 93, 12593–12598.
Moshkin, Y.M., Armstrong, J.A., Maeda, R.K., Tamkun, J.W., Verrijzer, P., Kennison, J.A., Karch, F., 2002. Histone chaperone ASF1 cooperates with the Brahma chromatin-remodelling machinery. Genes Dev. 16, 2621–2626.
Munakata, T., Adachi, N., Yokoyama, N., Kuzuhara, T., Horikoshi, M., 2000. A human homologue of yeast anti-silencing factor has histone chaperone activity. Genes Cells 5, 221–233.
Nonet, M.L., Staunton, J.E., Kilgard, M.P., Fergestad, T., Hartwieg, E., Horvitz, H.R., Jorgensen, E.M., Meyer, B.J., 1997. *Caenorhabditis elegans* rab-3 mutant synapses exhibit impaired function and are partially depleted of vesicles. J. Neurosci. 17, 8061–8073.
O'Connell, K.F., Leys, C.M., White, J.G., 1998. A genetic screen for temperature-sensitive cell-division mutants of *Caenorhabditis elegans*. Genetics 149, 1303–1321.
Parusel, C.T., Kritikou, E.A., Hengartner, M.O., Krek, W., Gotta, M., 2006. URI-1 is required for DNA stability in *C. elegans*. Development 133, 621–629.
Recht, J., Tsubota, T., Tanny, J.C., Diaz, R.L., Berger, J.M., Zhang, X., Garcia, B.A., Shabanowitz, J., Burlingame, A.L., Hunt, D.F., Kaufman, P.D., Allis, C.D., 2006. Histone chaperone Asf1 is required for histone H3 lysine 56 acetylation, a modification associated with S phase in mitosis and meiosis. Proc. Natl. Acad. Sci. U. S. A. 2, 6988–6993.
Sanematsu, F., Takami, Y., Barman, H.K., Fukagawa, T., Ono, T., Shibahara, K.I., Nakayama, T., 2006. Asf1 is required for viability and chromatin assembly during DNA replication in vertebrate cells. J. Biol. Chem. 281, 13817–13827.

Schulz, L.L., Tyler, J.K., 2006. The histone chaperone ASF1 localizes to active DNA replication forks to mediate efficient DNA replication. FASEB J. 20, 488–490.
Sen, S.P., De Benedetti, A., 2006. TLK1B promotes repair of UV-damaged DNA through chromatin remodeling by Asf1. BMC Mol. Biol. 7, 37.
Sharp, J.A., Fouts, E.T., Krawitz, D.C., Kaufman, P.D., 2001. Yeast histone deposition protein Asf1p requires Hir proteins and PCNA for heterochromatic silencing. Curr. Biol. 11, 463–473.
Sillje, H.H., Nigg, E.A., 2001. Identification of human Asf1 chromatin assembly factors as substrates of Tousled-like kinases. Curr. Biol. 11, 1068–1073.
Sulston, J.E., Horvitz, H.R., 1981. Abnormal cell lineages in mutants of the nematode *Caenorhabditis elegans*. Dev. Biol. 82, 41–55.
Sulston, J.E., Albertson, D.G., Thomson, J.N., 1980. The *Caenorhabditis elegans* male: Postembryonic development of nongonadal structures. Dev. Biol. 78, 542–576.
Sutton, A., Bucaria, J., Osley, M.A., Sternglanz, R., 2001. Yeast ASF1 protein is required for cell cycle regulation of histone gene transcription. Genetics 158, 587–596.
Tagami, H., Ray-Gallet, D., Almouzni, G., Nakatani, Y., 2004. Histone H3.1 and H3.3 complexes mediate nucleosome assembly pathways dependent or independent of DNA synthesis. Cell 116, 51–61.
Tamburini, B.A., Carson, J.J., Adkins, M.W., Tyler, J.K., 2005. Functional conservation and specialization among eukaryotic anti-silencing function 1 histone chaperones. Eukaryot. Cell 4, 1583–1590.
The *C. elegans* Sequencing Consortium, 1998. Genome sequence of the nematode *C. elegans*: a platform for investigating biology. Science 282, 2012–2018.
Tsubota, T., Berndsen, C.E., Erkmann, J.A., Smith, C.L., Yang, L., Freitas, M.A., Denu, J.M., Kaufman, P.D., 2007. Histone H3-K56 acetylation is catalyzed by histone chaperone-dependent complexes. Mol. Cell 25, 703–712.
Tyler, J.K., Adams, C.R., Chen, S.R., Kobayashi, R., Kamakaka, R.T., Kadonaga, J.T., 1999. The RCAF complex mediates chromatin assembly during DNA replication and repair. Nature 402, 555–560.
Umehara, T., Horikoshi, M., 2003. Transcription initiation factor IID-interactive histone chaperone CIA-II implicated in mammalian spermatogenesis. J. Biol. Chem. 278, 35660–35667.
Wormbase, (2005). http://www.wormbase.org.
Yamaki, M., Umehara, T., Chimura, T., HOrikoshi, M., 2001. Cell death with predominant apoptotic features in *Saccharomyces cerevisiae* mediated by deletion of the histone chaperone ASF1/CIA1. Genes Cells 6, 1043–1054.
Zabaronick, S.R., Tyler, J.K., 2005. The histone chaperone anti-silencing function 1 is a global regulator of transcription independent of passage through S phase. Mol. Cell. Biol. 25, 652–660.
Zhang, R., Poustovoitov, M.V., Ye, X., Santos, H.A., Chen, W., Daganzo, S.M., Erzberger, J.P., Serebriiskii, I.G., Canutescu, A.A., Dunbrack, R.L., Pehrson, J.R., Berger, J.M., Kaufman, P.D., Adams, P.D., 2005. Formation of MacroH2A-containing senescence-associated heterochromatin foci and senescence driven by ASF1a and HIRA. Dev. Cell 8, 19–30.